12-2013

Synthesis of a Bifunctional Heterogeneous Catalyst for the Conversion of Lignocellulosic Biomass into Precursors for Alternative Fuels and Fine Chemicals

Matthew David Dembo
University of Tennessee - Knoxville, mdembo@utk.edu

To the Graduate Council:

I am submitting herewith a thesis written by Matthew David Dembo entitled "Synthesis of a Bifunctional Heterogeneous Catalyst for the Conversion of Lignocellulosic Biomass into Precursors for Alternative Fuels and Fine Chemicals." I have examined the final electronic copy of this thesis for form and content and recommend that it be accepted in partial fulfillment of the requirements for the degree of Master of Science, with a major in Chemistry.

Craig E. Barnes, Major Professor

We have read this thesis and recommend its acceptance:

George K. Schweitzer, Brian K. Long

Accepted for the Council:
Carolyn R. Hodges

Vice Provost and Dean of the Graduate School

(Original signatures are on file with official student records.)

Synthesis of a Bifunctional Heterogeneous Catalyst for the Conversion of Lignocellulosic Biomass into Precursors for Alternative Fuels and Fine Chemicals

A Thesis Presented for the
Master of Science
Degree
The University of Tennessee, Knoxville

Matthew David Dembo
December 2013

Abstract

The overall goal of the research described here is to develop synthetic routes to bifunctional reagents that can be tethered into silicate matrices derived from the tin functionalized cube, $Si_8O_{20}(SnMe_3)_8$ [octatrimethyltin silicate]. The critical functional group required for reaction with cubic silicate building block is a chlorosilane, and we additionally wish to incorporate both acid and ionic liquid groups. Once in hand, a crosslinking metathesis reaction will incorporate these reagents into porous silicate matrices derived from the Si_8O_{20} [silicate] cube, creating platforms with both acid and ionic liquid groups tethered to their surfaces.

The synthesis of a family of bifunctional compounds containing silyl chloride groups "tethered" to either imidazolium-based ionic liquid groups or aryl sulfonic acid groups is described. The general synthetic strategy involved an initial platinum catalyzed hydrosilation coupling of an allylbenzene or 1-allyl-3-N-benzyl-imidazolium reagent to produce a silane group containing at least one chloride substituent. Sulfonation of the aromatic rings to produce sulfonic acid groups proceeds smoothly and in high yield with chlorosulfonic acid.

These reagents were subsequently reacted with the octatrimethyltin silicate cube, to produce cross-linked silicate matrices containing different combinations of tethered imidazolium groups and sulfonic acids to their surfaces. These functionalized solids were tested for catalytic activity in the hydrolysis of the cellulose model compound, cellobiose, and the dehydration of glucose to hydroxymethyl furfural or levulinic acid.

Table of Contents

List of Figures

Chapter 1: Introduction

Most petroleum consumers don't think twice about where their gasoline comes from, and likewise are oblivious to the geopolitical consequences of harvesting, refining, and trading oil. This is surprising given that the U.S. has a large influence in the production and consumption of petroleum based products. Many don't realize that the U.S. produces as much oil as Russia (more than 10 million barrels per day), and almost as much as Saudi Arabia, the largest producer in the Middle East at more than 11 million barrels per day. While this may seem impressive, our daily consumption of 18.8 million barrels per day is twice as much as the next largest world consumer, China, and means that we are still dependent on the importation of foreign oil at a cost of $1 billion per day to meet our nation's demands.[4] Furthermore, while the U.S. does keep a Strategic Petroleum Reserve (SPR) of 727 million barrels for emergency distribution, even with the largest reserve in the world, the U.S. would not be able to fully support its daily petroleum needs for an indefinite amount of time without importation from other nations. This is undesirable, as political volatility is often difficult to predict and slow to resolve itself.[5]

While gasoline is the first product that comes to mind for an oil consumer, it only accounts for 46% of a 42 gallon barrel of oil. As shown in Figure 1 below, 24% is processed to make diesel fuel, 9.3% for jet fuel, 4.1% for liquefied petroleum gas, and 4% to heavy fuel oil. This means that over 70% of a barrel of oil is used for transportation, with the rest contributing to residential and industrial heating and electricity, as well as energy to drive chemical processes for synthesis of plastics, industrial chemicals, and pharmaceuticals. Thus, in order to reduce or eliminate the U.S. dependence on petroleum, we must enhance or replace a major portion of our energy sources for transportation.[3]

Figure 2 shows that fossil fuels such as coal and natural gas make up the majority of the remainder of the U.S. energy sources. However, it is well known that, along with oil, these resources are not inexhaustible. This has led more recently to a shift towards renewable energy sources such as wind, solar, tidal, and geothermal technologies to generate electricity from naturally occurring forces, as well as conversion of biomass into chemical replacements for petroleum products. While biomass accounts for only a small portion of these renewable resources, it has the greatest potential for immediate development, as the resulting biofuels can be easily integrated into the existing infrastructure used to distribute petroleum based fuels to satisfy transportation demands; something not as easily accomplished by modern hydrogen based technologies. [2]

The term "biomass" refers to renewable biological materials, typically plant-based, which are composed almost entirely of carbon, oxygen, and hydrogen. While mankind has used combustion of these materials for centuries to generate energy in the form of heat, this process is not nearly as efficient as when hydrocarbons are used due to the large component of oxygen in biomass materials. A more recent approach to utilize widely available biomass sources that provides much greater efficiency is to chemically convert them into compounds that are more easily transported, stored, or utilized as biofuels. There are two general approaches to the conversion of biomass into biofuels, enzymatic fermentation or chemical transformation, as well as two major sources of agricultural feedstocks, discussed below, that lead to first generation or second generation biofuels.[6]

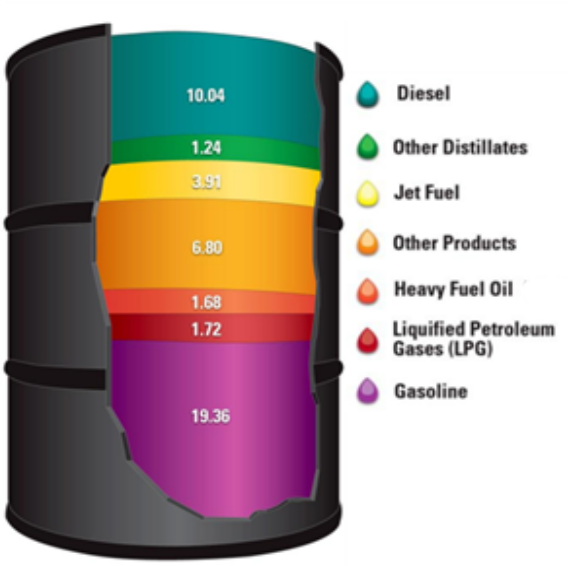

Figure 1: Products from a Barrel of Crude Oil. Numbers given are in gallons.[3]

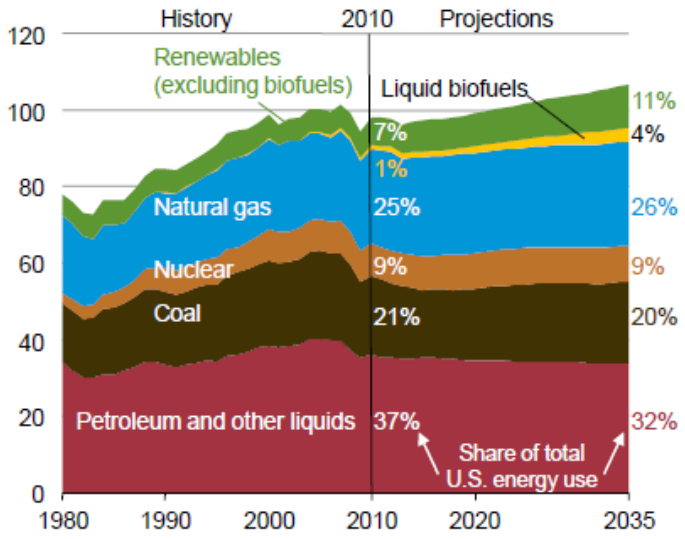

Figure 2: Energy Use by Fuel. Figures are projected to 2035 in quadrillion btu's.[2]

First generation biofuels are generated from sugars and oils, with sugarcane and corn as common starting materials. These crops are harvested and allowed to ferment, typically in the presence of added enzymes, to produce ethanol with an energy content of 23 MJ/L, which is used as a gasoline additive (gasoline contains 35 MJ/L). While these biomass sources are easier to process than second generation biofuels, they are also food stocks, meaning that use of these materials would create a competition between food and fuel, drastically raising the cost of these starting materials and rendering them economically nonviable on a large scale.

Second generation biofuels are generated from non-food crop feedstocks, such as agave[7] and bamboo[8] plants, as well as agricultural and forest residues and byproducts from paper mills and other sources. Utilization of these 'lignocellulosic biomasses' would provide an opportunity to recycle these materials which would otherwise be discarded as waste, as well as to make use of poorer quality land considered unsuitable for farming food crops. Additionally, these crops have a higher yield and shorter turnover time than those required for first generation biofuel feedstocks, which would greatly improve the production time and availability.[9]

Lignocellulosic biomass accounts for the majority of plant matter viable for conversion and is a complex polymeric system comprised of three major components: hemicellulose (25%), cellulose (40%), and lignin (25%). As seen in Figure 3 below, a plant cell wall is made up of sugar molecules that polymerize

together to make a cellulose microfibril which is wrapped in a layer of hemicelluloses and is further linked by strands of lignin.

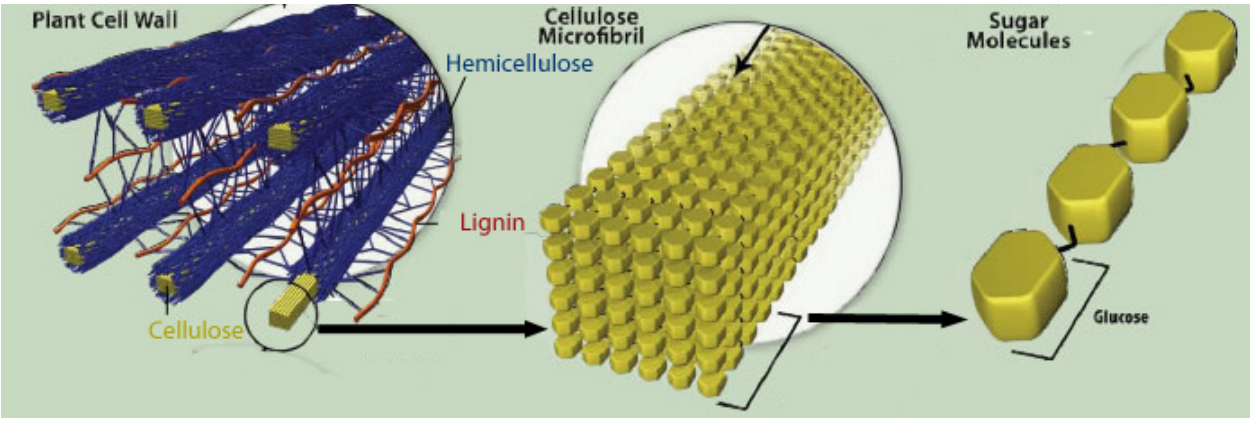

Figure 3: Cell Wall Composition. Includes major components cellulose, hemicellulose, and lignin.[10]

More specifically, cellulose is a polymer of glucose units linked by β-1,4-glycosidic bonds into tightly packed chains, resulting in a highly ordered crystalline structure that is water insoluble and resistant to depolymerization. Hemicellulose, a polymer composed mostly of the pentose sugar xylose along with other sugars, forms branched chains and is shorter than cellulose. While it forms hydrogen bonds to cellulose microfibrils, it has a random, amorphous structure with little strength and is easily hydrolyzed by acid. Finally, lignin, an aromatic organic polymer, adds additional strength, hydrophobicity, and some resistance to disease and pests for the plant. All three of these components have viable applications as precursors for the formation of biofuels, however this research will focus on the conversion of cellulose. The goal of this project is to develop a protocol for the simultaneous conversion of cellulose into both fine chemicals and fuels in an economically viable and efficient manner. This will be accomplished by using a specifically tailored solid acid catalyst designed to modify cellulose into a chemical precursor that can also be utilized in the synthesis of valuable fine chemicals, as well as undergo simple, direct conversion processes to petroleum based fuel replacements.

Chapter 2: Current Strategies

A lot of interest has focused on the use of 5-hydroxymethylfurfural (5-HMF) as a precursor for both fuel alternatives, as well as for fine chemical production. This compound, formed via selective dehydration of hexoses, can be further transformed into levulinic acid and 2,5-disubstituted furans derivatives, as shown in Figure 4 below. Levulinic acid is a precursor to nylon-like polymers, synthetic rubbers, and plastics, as well as a versatile intermediate for pharmaceutical synthesis, while the furans serve as building blocks for the production of plastics and fine chemicals. 2,5-dimethylfuran (DMF), obtained by hydrogenation of 5-HMF, is of particular interest as a fuel alternative, as it has an energy content of 31.5 MJ/L (compared to gasoline at 35 MJ/L), is less volatile than ethanol (23 MJ/L) and is immiscible with water. While high-yield procedures exist for the conversion of fructose into 5-HMF by acid-catalyzed dehydration, fructose is a costly starting material. Glucose, on the other hand, is very low cost and widely available, due in large part to the current underutilization of cellulose.

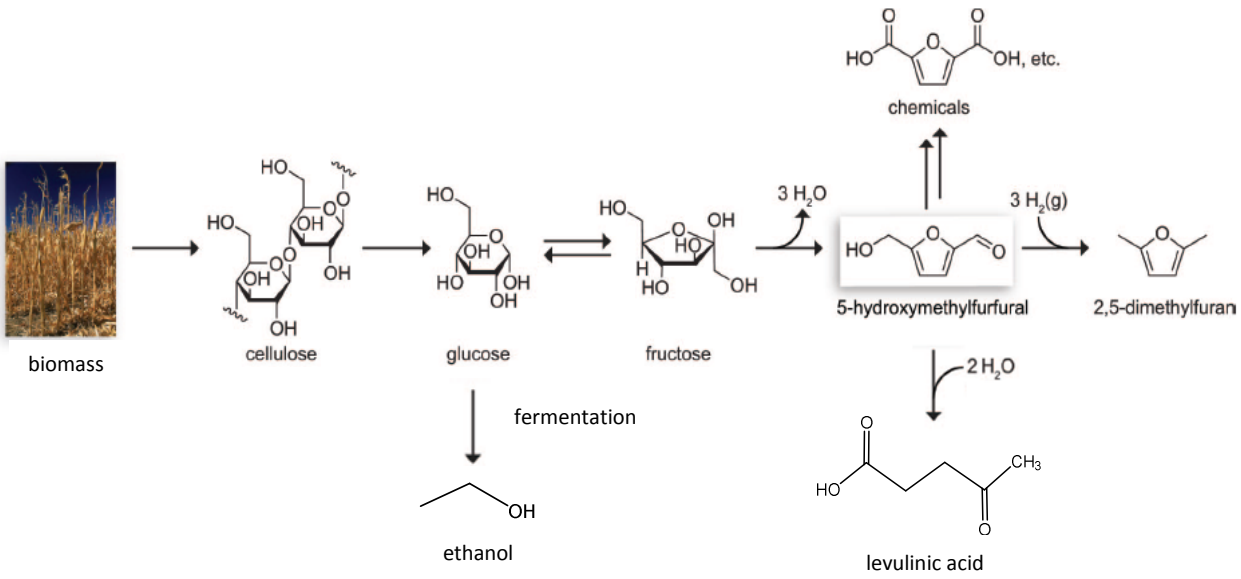

Figure 4: Pathway for conversion of biomass into fine chemicals and fuel alternatives. [11]

One of the most challenging aspects of the conversion of lignocellulosic biomass is its resistance to assaults from its natural environment; a resistance which also extends to synthetic chemical conversions. The reasons for this are: (1) waxy barriers and dense cells separating the plant from its external environment, (2) vascular structure of plants that limit liquid penetration into plant stems, (3) composite nature of plant cell wall which restricts the penetration of liquids between cells and limits available surface area, largely a result of lignin (4) the sheathing of the cellulose microfibrils by hemicellulose, and (5) the crystalline nature of cellulose itself.[12] Combinations of these factors are responsible for the resistance of these materials to chemical conversion via hydrolysis, termed

'recalcitrance', and create the need for costly pretreatment steps before the biomass can be efficiently processed.

The goal of a pretreatment process is to alter or remove structural impediments for the hydrolysis of cellulose into oligomers in order to improve the rate of reaction. This process aims to break the lignin seal, to disrupt the hydrogen bonds of the hemicelluloses sheath and dismantle it into pentoses, as well as to disorder the crystalline structure of cellulose to make it more vulnerable to hydrolysis into glucose. These modifications can be achieved through several chemical approaches, such as steam explosion, liquid hot water, lime, and ammonia or acid pretreatments. The hydrolysis of untreated biomass shows typical glucose yields from around 20%, but this increases up to 90% and higher for pretreated biomass. Of the four traditional enzymatic conversion steps (pretreatment, hydrolysis, fermentation or chemical conversion, and product separation and purification), pretreatment is the most expensive.[13]

Recently, the ability of ionic liquids to solubilize lignocellulosic biomass has been described. Ionic liquids are salts that are commonly liquid at room temperature and have several unique properties. These compounds often contain an organic heterocycle, such as imidazolium or pyridinium salts as illustrated in Figure 5 below, and can be tuned to have nonpolar or polar, acidic or basic, or H-bond acceptor or donor functionalities by altering the counterion and side chain as necessary. These salts tend to be highly viscous, have a very low vapor pressure, show excellent thermal stability relative to other organic compounds, and are most commonly employed as unique solvents.[14]

As applied to conversion of lignocellulosic biomass, it has been suggested that the counterion selection is of utmost importance, such that a weakly ion-paired selection is most effective at solubilizing biomass.[11] It is thought that the weak interaction of the counterion with the cationic ring allows for the anion to easily dissociate, preferring instead to interact with the hydrogen bonding network prevalent in cellulose and hemicellulose. This interaction disrupts the structural integrity of the lignocellulosic materials, and leads to both depolymerization of the cellulose and hemicellulose polymers, as well as disordering of the natural crystallinity of cellulose, leaving it more susceptible to further chemical breakdown, as well as greatly increasing its solubility.[15] These effects allow ionic liquids to act as both pretreatment and solvent for the reaction, eliminating a costly step. At the same time, they are considered quite expensive and are difficult to separate from the reaction mixture, leading to low reusability.

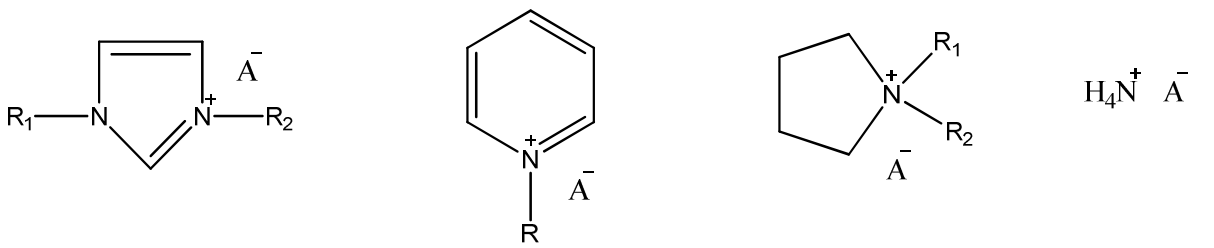

Imidazolium Pyridinium Pyrrolidinium Ammonium

Figure 5: Common ionic liquid structures with varying R-groups and anions (A^-).

Whereas α-glucose is easily obtained through degradation of amylase, a helical polymeric structure that makes up a large component of starch, the β-glucose anomer is what is obtained from the breakdown of the more resilient cellulose polymer, as displayed in Figure 6 below, and will be the target of the proposed conversion process. Once lignocellulosic biomass has been decrystallized, the hydroxyl groups and β-glycosidic linkages of cellulose will be exposed. This leaves it much more vulnerable to the hydrolysis reactions necessary to depolymerize it into small oligomers in order to isolate the monosaccharide components. Homogeneous catalysts are frequently used on account of their dissolution in the reaction medium to facilitate an interaction with the solid biomass, as well as the fact that they tend to require milder reaction conditions while remaining very selective. However, solid catalysts are still preferred in industry, with an estimated 80-85% of these chemical processes employing the use of solid catalysts.[16]

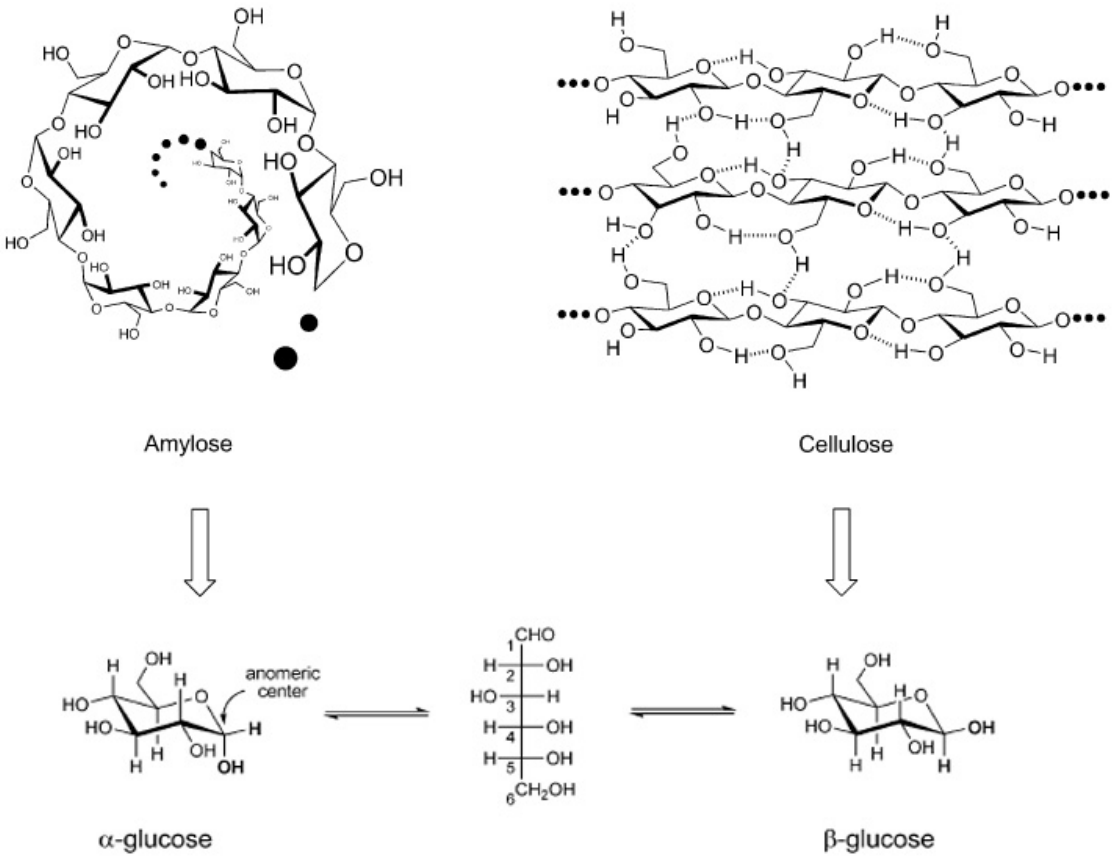

Figure 6: Polymeric Forms of glucose and its anomeric constituents.[17]

A major reason that solid catalysts are preferred in industry is the fact that they can be easily recycled. This is due to the straightforward separation from reaction products, since separation processes are a large expense for the chemical and fuel industries representing more than half of the total investment in equipment.[18] Hydrolysis reactions to cleave the glycosidic bond, the C–O–C linkage between glucose monomers, are typically carried out in the presence of acid catalysts between 370 K and 570 K, as base hydrolysis produces more side reactions.[19] Given the advantages of heterogeneous catalysis, solid acids are often employed in this reactions, with the acid functionality incorporated into several varying solid support systems, including but not limited to zeolites[20], ion-exchange resins[15], metal phosphates[21] and metal oxides[22], as well as sulfonated silica[23], aluminum[8] and zirconia species. While each system has its own advantages and disadvantages, no one system has been proven significantly more effective than another.

The isomerization of glucose to fructose is an important industrial process used in the formation of high fructose corn syrup, however it relies on biological enzymes which require precise maintenance of pH and temperature to prevent denaturing that destroys the enzymatic structure and thus its activity.[24] Although genetic engineering of plants or microorganisms can overcome these limitations to increase

the overall yield of an enzymatic conversion process, it adds additional costs to the utilization of biomass, decreasing its overall economic viability with respect to fossil fuels. While this process occurs naturally, it is somewhat sluggish and can be sped up by implementation of high temperature and presence of a base to allow for proton transfer, or a metal center with open coordination sites to facilitate an intramolecular hydride shift, as shown in Figure 7B below.[25] The most common approach is to use a metal oxide and recent evidence suggests this can be enhanced in the presence of water with microwave exposure[26], however the use of metal chlorides in combination with an ionic liquid solvent has also shown to be effective[27]. Regardless, the rate of glucose isomerization is dictated by the fraction of glucose molecules in the open-chain form. This is higher in aprotic solvents, such as DMSO, as well as at higher temperatures typically around 350 K.[28]

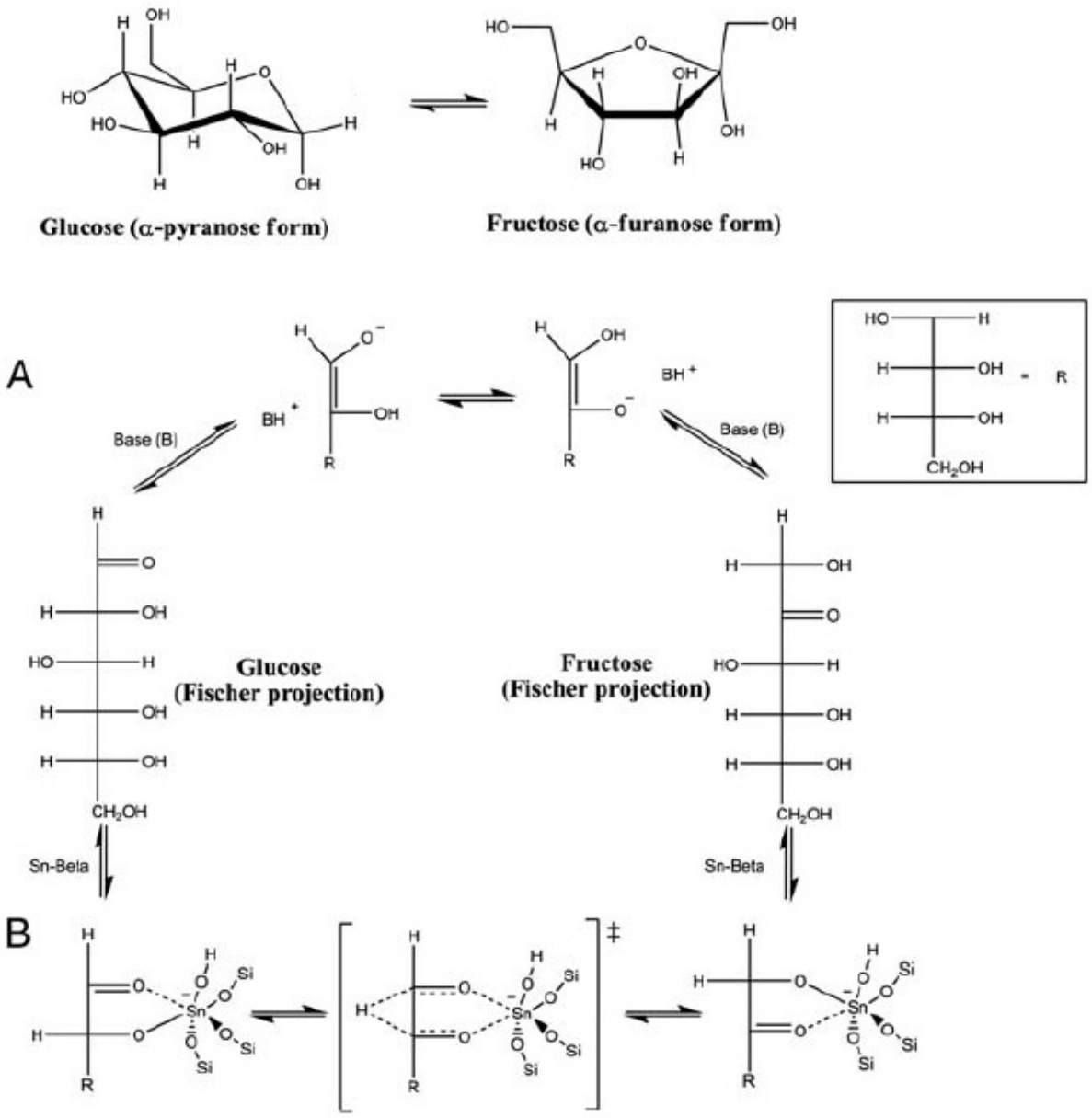

Figure 7: Glucose isomerization mechanism by A) base catalyzed proton transfer and B) metal catalyzed intramolecular hydride shift.[29]

Once fructose has been isolated, it can be directly converted into the target product, 5-HMF. This involves the loss of three equivalents of water in an acid-catalyzed dehydration reaction, and is more selective towards ketohexoses like fructose than aldohexoses like glucose. While glucose can technically undergo the same reaction, it is well known that higher rates and selectivities are achieved for the dehydration of fructose into 5-HMF, such that it is more economically viable to force isomerization from glucose to fructose before dehydration rather than attempt dehydration of glucose directly.[30] If kept in

the presence of water, HMF can rehydrate into levullinic acid and formic acid, and if excess fructose remains, HMF will react through a condensation process. This is sometimes countered by using a biphasic solvent system, such that the HMF created is immediately extracted into an organic phase to keep it separated from water and fructose, however given its poor partitioning, a large amount of extracting solvent is required and oftentimes the energy needed to purify the diluted HMF is not economical.[31] This has been demonstrated with some success in a water/DMSO biphasic system, where the addition of poly(1-vinyl-2-pyrrolidinone) (PVP) into the aprotic extraction phase acted as a modifier to help suppress the formation of byproducts .[30]

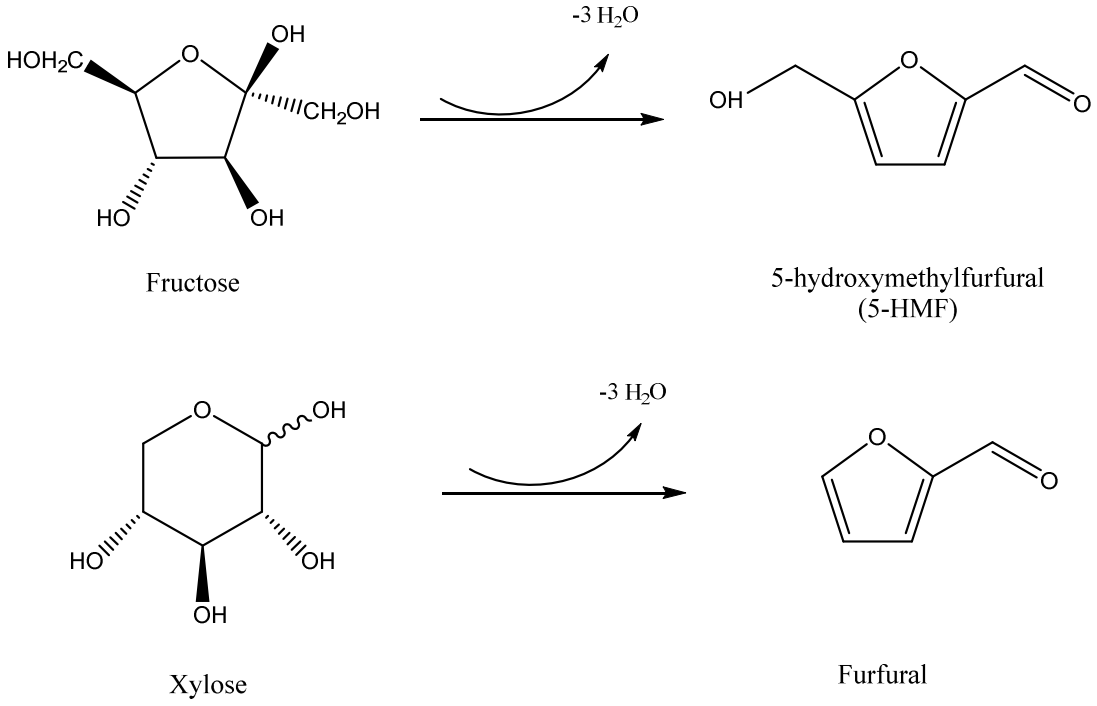

Figure 8: Dehydration of cellulose-derived fructose into 5-HMF and hemicellulose-derived xylose into furfural.[32]

There are many value-added transformations that can be applied from furan precursors to yield diesel fuel additives, industrial solvents, bioderived polymers, P-series fuels (by hydrogenolysis of furfural), and so on. Given the potential for glucose derived from a cheap, abundant lignocellulosic biomass source, many new doors would open given the right multifunctional catalyst that could handle several of these reactions in a one-pot process with limited use of solvents.

Chapter 3: Proposed Research

The conversion of cellulose into an ideal precursor susceptible to both value added synthesis of fine chemicals and facile processing into potential alternative fuels is a daunting task, both because of its physical nature and as a result of the numerous consecutive reactions that must occur. The recalcitrant nature of cellulose must first be overcome to leave its structural foundations and chemical functionalities vulnerable to further modification. Once these have been exposed, hydrolysis will effect the permutation of individual cellulose chains into dimeric cellobiose and glucose monomers. Then, while glucose can be directly dehydrated into 5-hydroxymethylfurfural, the target intermediate compound, yields and selectivity will be much higher if an isomerization to fructose is employed before dehydration. To combine all of these processes into a one-pot reaction that can utilize a single catalyst and solvent system is quite challenging, especially given the evolution of reactants from polar compounds with a high oxygen to carbon ratio into nonpolar products with a low O/C ratio as the reaction proceeds. However, both hydrolysis and dehydration processes are acid-catalyzed reactions, which suggests the use of an acidic functionality in the design of the proposed catalyst. The versatility of solid acid catalysts, illustrated in Figure 9 below, lends itself well to this particular application, as the reactions they effect are as varied as the myriad of biomass that they may be applied to.

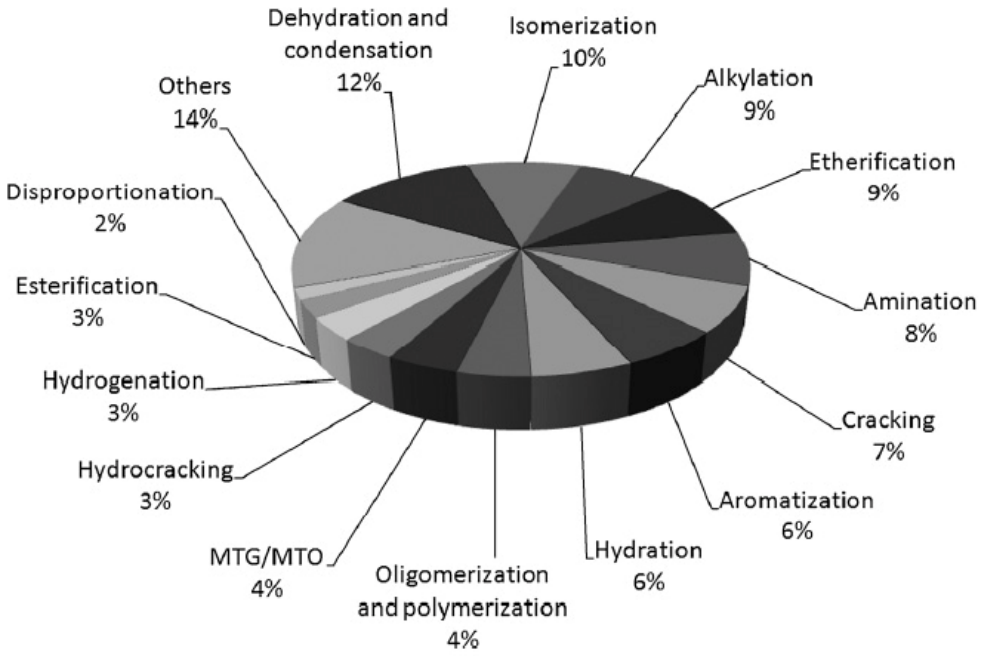

Figure 9: Utilization of solid acid catalysts in chemical processes. [33]

While ionic liquids are a viable option for solving the recalcitrance problem due to their ability to dramatically improve the solubility of biomass, they are expensive to produce and very difficult to purify and reuse. However, we believe that they are critical in directing the interaction of the solid acid sites with biomass, a process that is otherwise troublesome as solid-solid interactions are inherently difficult to facilitate. Thus, they serve to enhance the interaction between the biomass substrate and the active acidic site where catalysis of the hydrolysis and dehydration reactions occur. To compensate for their cost and reusability, we propose a strategy to tether both an ionic liquid and an acid functionality to a solid silicon support matrix such that heterogeneous catalysis can be practically performed, making separation of the tethered ionic liquid from the liquid products much easier, and allowing for its reuse.

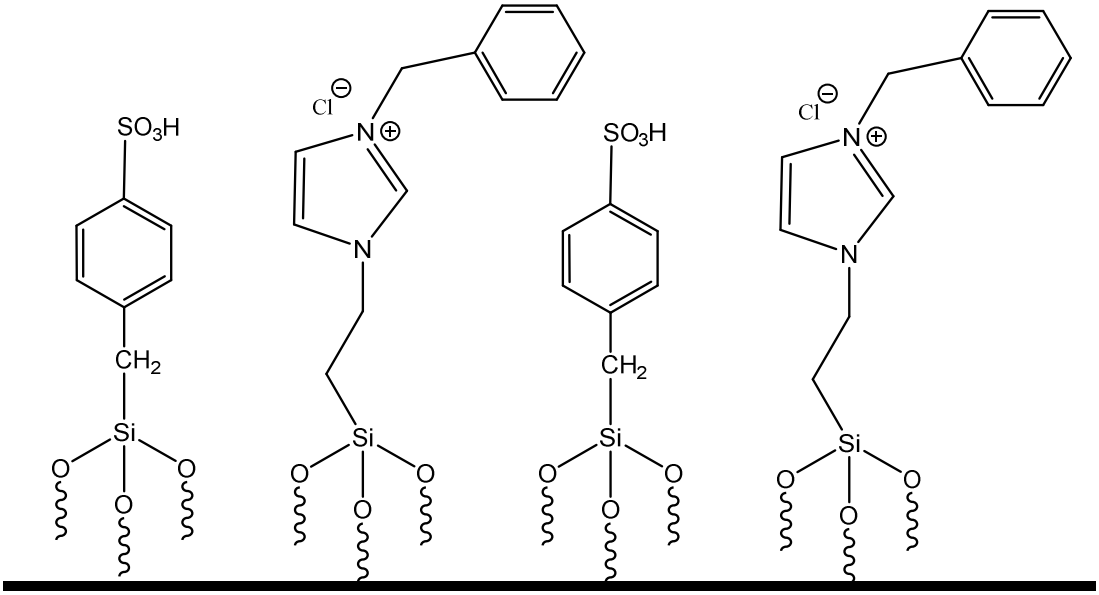

Figure 10: Tethering an ionic liquid and acidic functionality to a solid support.

This approach combines two lines of reasoning: first, that ionic liquids interact strongly with and solubilize cellulosic material, and second, solid acid catalysts hydrolyze cellulose into monosaccharides. Tethered ionic liquid groups will ideally overcome the natural recalcitrance of biomass and help deliver the active acid sites to the linkages that we wish to hydrolyze. This 'trojan horse' approach would solubilize cellulose using the ionic functionalities to disrupt the hydrogen-bonding network in cellulosic material and effectively depolymerize it to small molecules that are then more easily hydrolyzed by acidic functionalities contained within the same catalytic platform.

There are several key features that will need to be incorporated into such a catalyst to accommodate for both attachment of the necessary functionalities, as well as interaction with and activity towards the targeted lignocellulosic substrate. While zeolites and metal oxides account for over 70% of solid materials as catalysts in chemical industry,[33] biomass is a unique substrate that demands special considerations. A major difference is the size of the molecules that are formed during the processing of lignocellulosic biomass. While β-glucose measures 0.58 by 0.50 by 0.57 nm and can access the less than 2 nm micropores of zeolites easily, when the dimensions are expanded to a single chain of cellulose containing approximately 1000 β-glucose units, that length increases to 580 nm, which falls into the realm of macropores loosely defined as >50 nm.[34]

It is important to note that the hydrolysis reaction must occur to some extent before the pores can be accessed by the resulting species, since hydrolysis is an acid-catalyzed reaction required to initiate the following defunctionalization reactions. Therefore, it is crucial that the post-solvated, noncrystalline glucose chains have access to the acidic sites of the catalyst. This can be accomplished either through the reversible release of H^+ by a Brønstead acid into the reaction medium to act through homogeneous catalysis towards solubilized cellulose,[35,36] or by creating an active site on an easily accessible surface to permit heterogeneous catalysis. Regardless, something entirely nonporous is also not ideal, as surface area is directly related to activity rate and a high specific surface area (SSA) will help provide additional sites of reaction for the subsequent dehydration reaction on the same catalyst. Additionally, porosity can help increase yields of the reaction through reagent, product, or transition state selectivity achieved by specifically tailoring the size of the pores such that they are only accessible to certain molecules, especially when isomerization to fructose is not emphasized.

Furthermore, in addition to the catalyst requiring acidic functionalization, several biomass components contain acidic and chelating compounds, which facilitate leaching and poisoning of traditional zeolitic or metal oxide catalysts. These challenges can be circumvented by implementation of a more stable support matrix, such as carbon or silicon, which are resistant to chelating and acidic media. The Barnes group has spent the past several years developing a building block methodology for the formation of such a rigid, porous silicon support matrix that contains only a single type of active site and can be structurally tailored to accommodate its intended application. This process is dependent on three major constituents; (1) the building block, (2) the linking agents, and (3) the cross-linking reactions.

The building block is a spherosilicate octaanion, $Si_8O_{20}^{8-}$, which has been capped at the corners by trimethyl tin groups to form a stable, tin functionalized, spherosilicate, $Si_8O_{12}(OSnMe_3)_8$. Shown in Figure 10 below, this structure will herein be referred to as trimethyl tin cube, TMT cube, or tin cube.

Linking agents are used to connect the spherosilicate monomers together into an amorphous matrix. In this manner, specific attributes can be incorporated into the cube matrix as needed for the target substrate. For example, much work has been done incorporating high valent metal halide ligands, such as $AlCl_3$, $GaCl_3$, BBr_3, $TiCl_4$, $VOCl_3$, VCl_4, WCl_6, $WOCl_4$, and $SnCl_4$ as catalytically active sites. Linkers such as $SiCl_4$, $HSiCl_3$, $HSiMeCl_2$, Me_2SiCl_2, and Me_3SiCl which show no catalytic activity towards reactants have also been examined, for they can serve as inert crosslinking agents that further increase the rigidity, stability, and surface area of the matrix. These inert linkers can also be used to tune hydrophobicity of

the matrix, as using $SiCl_4$ will yield a much more hydrophilic system compared to insertion of Me_2SiCl_2 when they system is hydrolyzed to yield Si-OH groups.

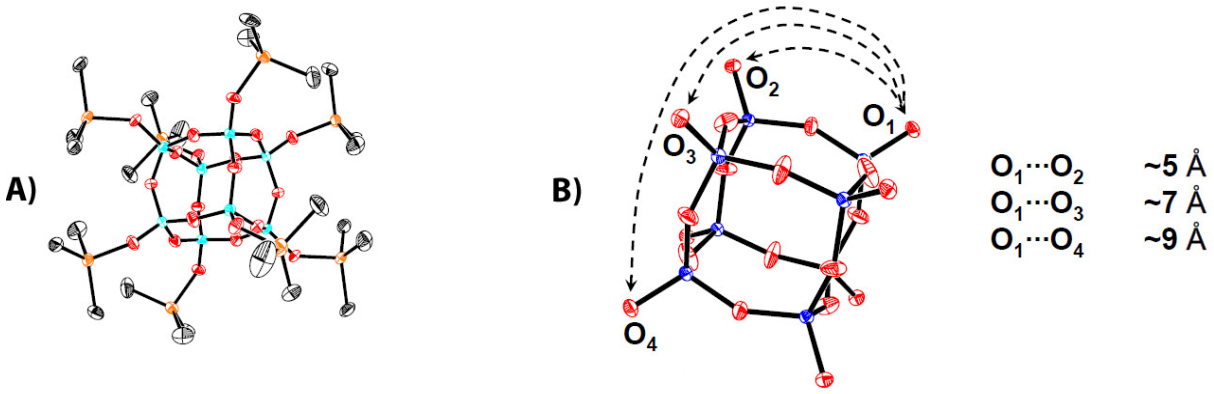

Figure 11: A) Illustrations of the trimethyltin cube. Red=O, Teal = Si, Orange = Sn, Grey = CH_3. B) Diagram showing the core Si_8O_{20} structure with linking point separation distances of terminal oxygens.

Altering reaction stoichiometry so that either the cube or linker is limiting during the cross-linking process allows one to control the connectivity of the linker to surrounding cubes. When a limiting amount of linker is used in the reaction, the trimethyltin groups on the corner of the cube will have access to all of the halide ligands and the linker will reach full connectivity to the cube such that it becomes embedded within the cube matrix. In contrast, limiting the availability of cube means that the halide groups on the linkers will be competing with one another for points of attachment to the cube, and they will reach connectivity less than the initial number of halides attached to the linkers to yield an exposed surface site.

The final part of the building block methodology is the cross-linking reaction itself. The trimethyltin caps serve as good leaving groups, allowing broad functionalization of the corners with either metal or silicon halides as previously described to produce trimethyltin chloride (Me_3SnCl) as a volatile byproduct via a metathesis reaction to yield M(Si)□O□Si bonds, shown in Figure 12 below. The size, shape and rigidity of the building block ensures that no two catalytic sites will be closer than 5-7 Å, which guarantees that the catalytic sites remain isolated, such that metal oxide domains do not form to yield multiple types of active sites. This methodology has several advantages not inherent to other synthetic techniques; it is a non-aqueous, non-hydrolytic, sol-gel condensation process that avoids templating agents, exclusively follows soft synthetic techniques, and is resistant to degradation via acid or temperature, as well as leaching.

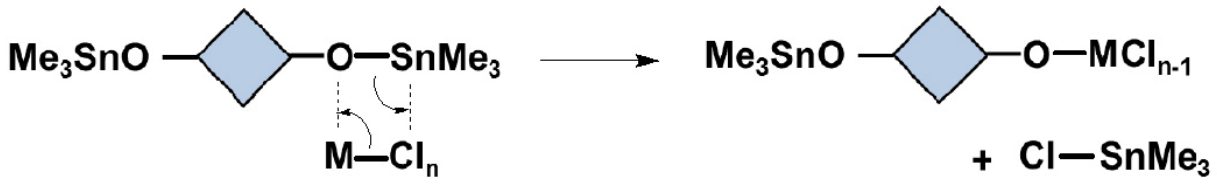

Figure 12: Cross-linking metathesis reaction, liberating Me_3SnCl as a volatile byproduct.

A catalyst tailored to tackle the task of biomass degradation will require a specially functionalized linking agent to cross link the cube support matrix. Already mentioned are the necessities to include both an acidic functionality, as well as an ionic liquid group. Finally, it would be advantageous for the linking agent to include an alkane tether to the solid support, such that the active acidic and ionic liquid sites remain flexible and mobile as if they were in a fluid environment. This design intends to combine the advantages of activity rates seen in homogeneous catalysis and the ease of separation observed in heterogeneous catalysis.

1-Allylimidazole (1-All-Im) is easily functionalized into a variety of imidazolium ionic liquids by reaction with compounds such as methyl iodide (MeI), benzyl chloride (BzCl), or hydrochloric acid (HCl). These reactions involve the creation of a cationic center at the free nitrogen of the imidazole ring, and the retention of the anionic component to balance the charge that is created in the alkylation reaction. Given the possible variation in ionic additives, the functionalization of the imidazole is nearly limitless and will allow for the catalyst to be tailored to meet the demands of its intended application, however this proposal will consider only those specifically mentioned above.

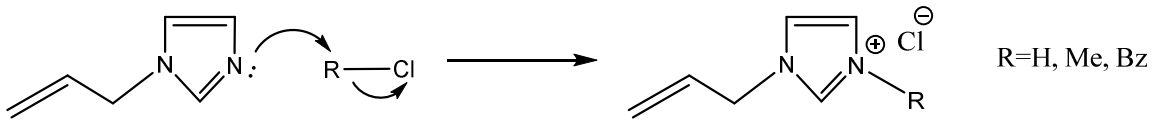

Figure 13: Conversion of 1-allylimidazole to an imidazolium chloride via addition of ionic salt.

As shown by the reaction of **2** to **3** or **4** in Figure 15 below, once the ionic liquid functionality has been created, it is possible to either continue to functionalize the linking agent to create an active acidic site (**2** to **3**), or focus on the addition of a silicon based point of attachment where the solid support matrix

will connect to the linker (**2** to **4**). Given the reactivity of a carbon-carbon double bond, it would be advantageous to first add a silane across the double bond before further modification to prevent unwanted side reactions. This is accomplished via a hydrosilation reaction in the presence of a platinum catalyst, and only requires one hydrogen on the silicon atom; the other three may vary, again allowing for the creation of several variations of the same catalytic framework.

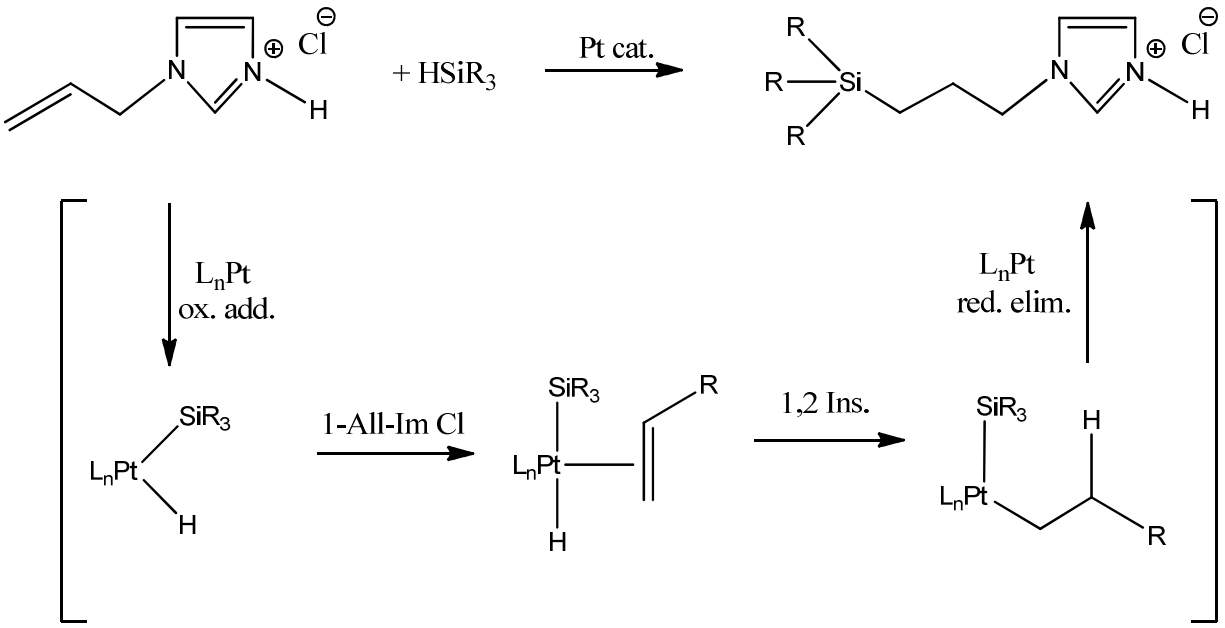

Figure 14: Mechanism for hydrosilation of 1-All-Im Cl to form a silylated propylimidazolium chloride.

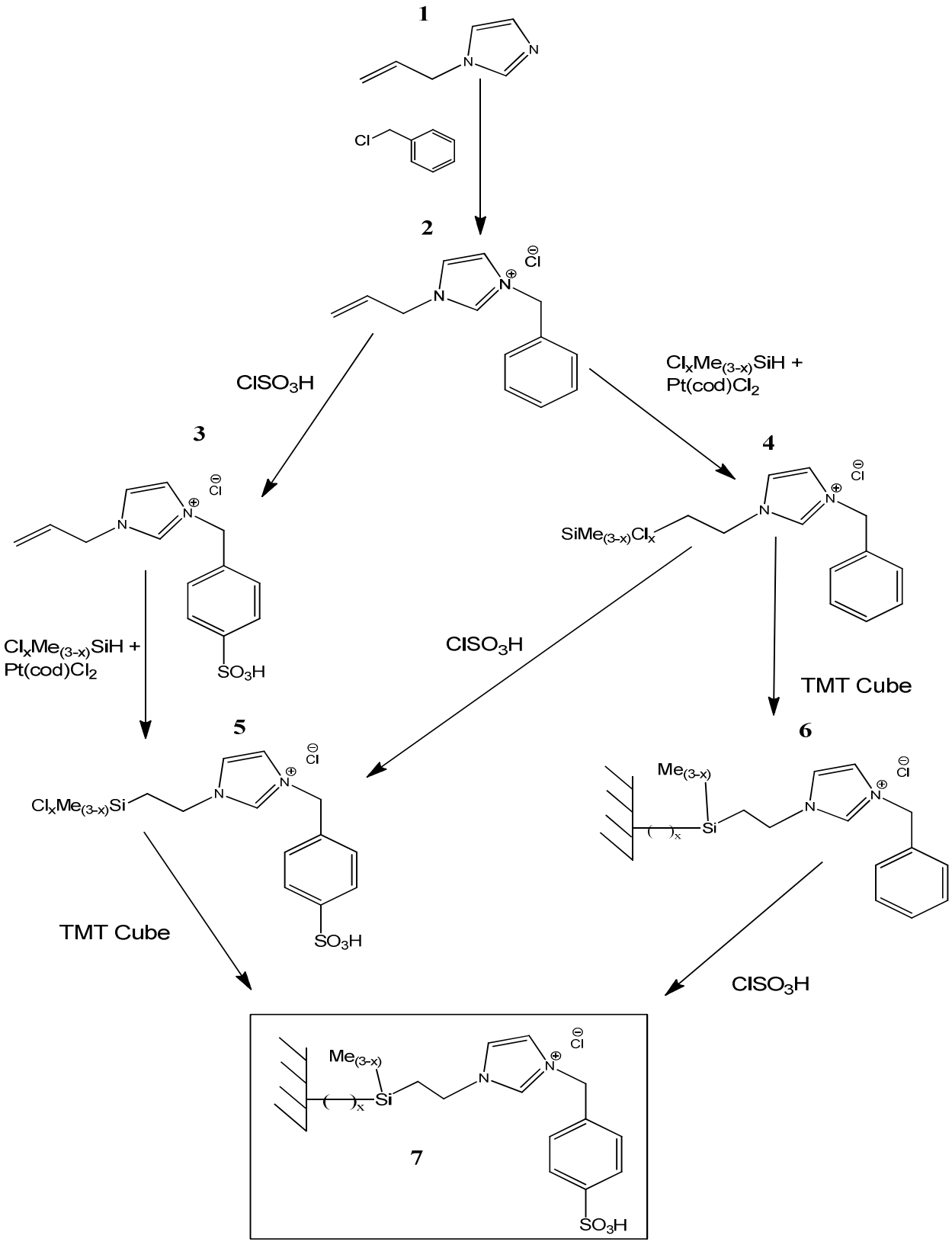

Figure 15: Potential reaction progressions for allylbenzene with benzyl chloride.

After hydrosilation, one can create an acidic functionality via sulfonation (**4** to **5**, Figure 15 above); however cross-linking the ligand with the cube matrix prior to sulfonation remains a viable option (**4** to **6**).

The cross-linking reaction is expected to yield a solid product that could be difficult to characterize with many spectroscopic techniques. It may therefore be more advantageous to proceed with sulfonation first to allow for more thorough characterization of the reaction product. The literature show a few options for this functionalization, including the use of hydrogen peroxide to oxidize a thiol group, □SH, to form a sulfonic acid group, □SO_3H,[37] or the ring opening reaction of a sultone[38]. A more aggressive option is to reflux with sulfuric acid at high temperatures, in contrast to a milder procedure using chlorosulfonic acid at low temperatures[39] (**2** to **3** above). Given the complexity of the linker needed for the cross-linking reaction, using the softer chlorosulfonic approach reduces the chance of disrupting its intended configuration. This reaction yields a □SO_3H moiety, as well as hydrochloric acid, HCl, as a byproduct. It is suspected that the HCl may be reactive towards remaining □$OSnMe_3$ groups, however it will be difficult to selectively scavenge since chlorosulfonic acid is used as a reactant. It is hoped that washing the product with an appropriate solvent or two may remove any remaining free soluble acids, leaving the tethered groups intact for catalysis. If HCl cannot be separated from the active catalyst, the results of catalysis may be falsely attributed to the active catalyst, when in fact it is the presence of excess HCl that catalyzes the biomass conversion reactions.

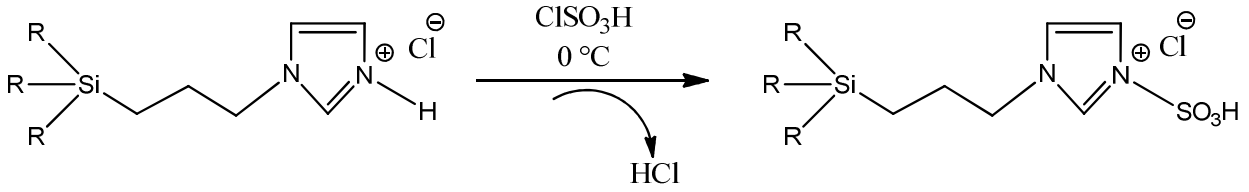

Figure 16: Sulfonation reaction with chlorosulfonic acid, $ClSO_3H$.

Once the entire linking agent has been successfully constructed, it should behave similar to any other inert linker in a cross-linking reaction with the tin cube. After the metathesis reaction, one would expect to see trimethyltin chloride, Me_3SnCl, as the sole volatile byproduct which can be confirmed by NMR spectroscopy. Additionally, gravimetric calculations can be used to monitor the ratio of Me_3SnCl that is lost with respect to the amount of linking agent added, such that the number of chlorides on the linking agent that have reacted can be quantized. This calculation yields the connectivity, or number of points through which the linker is actually connected to the solid support, and will vary depending on the number of halides attached to the linking agent prior to the cross-linking reaction. The connectivity also dictates how much of the linker is constrained through attachments to the support or hanging free in

space, and will determine if the linked group is embedded inside of the support matrix or exposed as a surface site.

A few modifications must be made before the catalyst can be effectively employed to assist in the conversion of lignocellulosic biomass. An important step is to improve the stability of the catalyst, such that it may be recycled for a number of reactions without degradation. Passivating the catalyst drastically improves its stability when in contact with air and moisture as is commonly the case in large scale catalytic applications. Passivation, exemplified in Figure 16 below, refers to the removal of residual groups that are highly reactive, including the trimethyltin groups on the corners of the cube building block, as well as Si□Cl bonds on a linker that may have failed to react during the cross-linking process. Si□Cl groups are especially sensitive to water, reacting in a manner similar to MeOH. The generation of HCl would likely complicate the processes for which the catalyst is tailored to function, and it is therefore beneficial to remove remaining Si□Cl groups prior to catalysis to prevent this. In a similar fashion, trimethyltin makes a very good leaving group and is prone to side reactions, making it disadvantageous to leave residual □OSnMe_3 groups on corners of the cube.

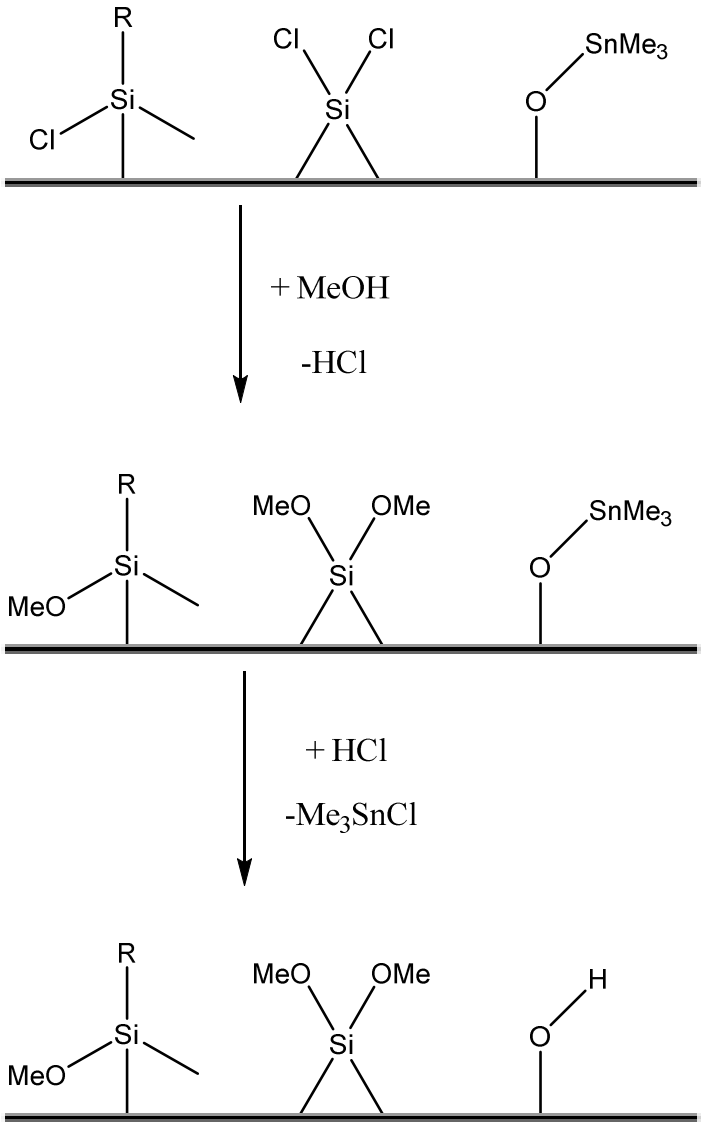

Figure 17: Passivation of residual reactive groups to improve stability of the catalyst.

Following passivation, water washings can be used to remove loosely associated soluble acids. By monitoring changes in pH of the washings, one can develop a sense for when the majority of free acid has been removed. At this point, the catalyst would be ready for implementation in a catalytic reactor, however it would be beneficial to characterize the acid sites in order to predict the behavior of the catalyst.

A common method for characterization of acid sites is temperature programmed desorption (TPD)[1]. This technique monitors the reaction of an amine, R-NH_2 with an acid as temperature is gradually ramped up, yielding ammonia, NH_3, in an elimination process. Isopropylamine is most commonly

employed as the reactant, yielding ammonia and propylene as products from the elimination reaction catalyzed by Brønsted acid sites as shown in Figure 17. These are monitored with gas chromatography – mass spectroscopy (GC-MS), where the area of the propylene signal is compared to the peak area for a known amount of a standard in order to estimate the concentration of acid sites that have reacted with the amine.

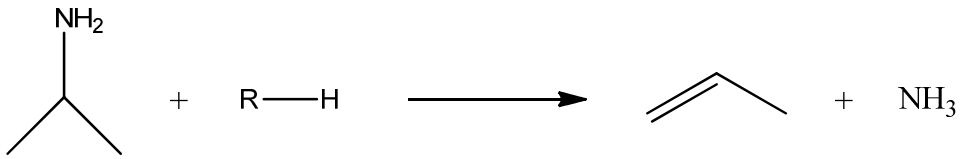

Figure 18: Elimination reaction between isopropylamine and an acid.

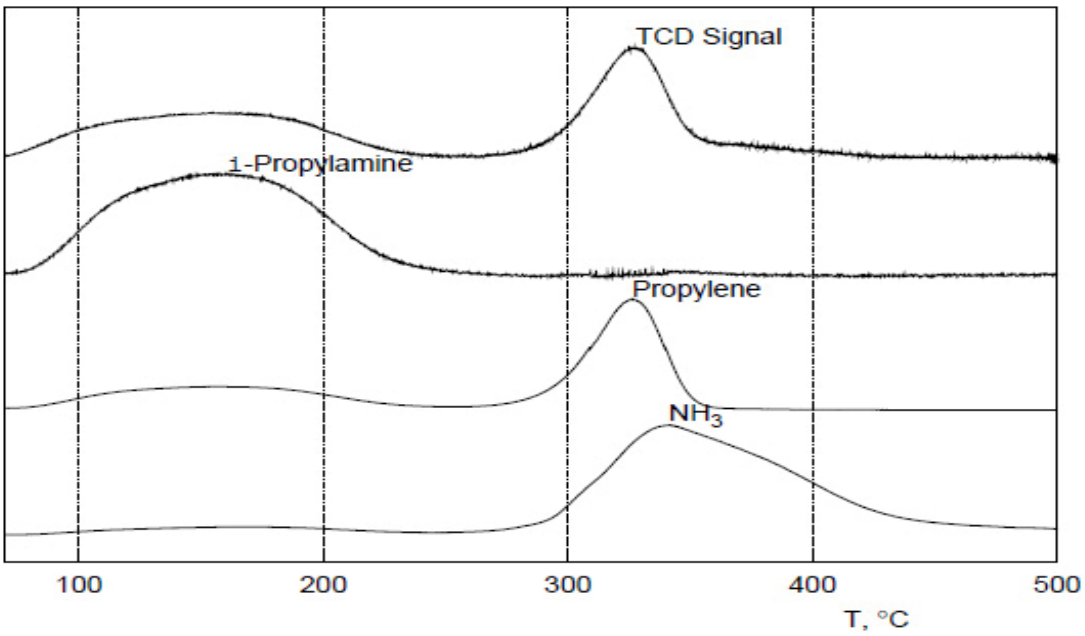

Figure 19: Deconvolution of GC-MS peaks from analysis of TPD volatiles.[1]

Chapter 4: Discussion of Results

Part 1: Experimental

Materials and Methods.

All starting reagents were purchased from Acros (organics), Gelest (silanes), or Strem (platinum, tin) and were either used without further purification or purified as described below.

All reactions were performed using standard Schlenk line techniques. Additionally, glassware was treated with a chlorotrimethylsilane/triethylamine/methylene chloride solution in order to remove reactive surface hydroxyls prior to reaction setup.

Hexane and toluene (Fisher Scientific) were distilled from sodium/potassium alloy (Na/K) and stored under vacuum in Schlenk bulbs containing Na/K. Methylene chloride and trichloroethylene (Fisher Scientific) were distilled from calcium hydride and stored under vacuum in a Schlenk bulb containing more calcium hydride. Pyridine and acetonitrile (Fisher Scientific) were distilled and stored over 4Å molecular sieves.

Chlorodimethylsilane ($HSiMeCl_2$) and trichlorosilane ($HSiCl_3$) were distilled, degassed, and stored under vacuum in Schlenk vessels.

Tetraethylorthosilicate (TEOS, $Si(OEt)_4$, Acros, 98%) was distilled and stored under nitrogen. Tetramethylammonium hydroxide (Me_4NOH, Acros, 25 wt% in MeOH) was used as received. Trimethyltin Chloride (Me_3SnCl, Strem, >98%) was verified via ^1H NMR and then used as received.

Gravimetric Analysis. The reaction flask was weighed empty, after the addition of each reactant, and after drying the reaction products. All measurements were carried out with the reaction flask under vacuum. The mass difference between the initial reactants and the final product was used to calculate the amount of Me_3SnCl lost, and thus the degree of cross-linking. It is important to note that the scale of the reaction must be large enough that the change in mass as a result of loss of Me_3SnCl is large enough to measure on a laboratory balance. Generally the variability in consecutive weighing on such scales is on the order of 3-5 mg, and as a result reactions with a predicted weight change of less than 50 mg are not recommended.

Nitrogen Adsorption. Surface area analyses were performed using the BET (Brunauer-Emmett-Teller) method. Data were collected on a Quanta Chrome Corporation Nova 1000 High Speed Surface Area and Pore Size Analyzer using nitrogen as the adsorption gas. The adsorption portion of the isotherm was used to calculate surface area.

Nuclear Magnetic Resonance Spectroscopy (NMR). Solution NMR spectra were collected at 9.4 Tesla on a Bruker Avance wide-bore NMR spectrometer utilizing a broadband inverse probe. ^1H, and ^{13}C spectra were acquired at 400.00 MHz and 100.60 MHz, respectively. Chemical shifts were referenced externally to 1H NMR δ [$CDCl_3$, D_2O]: 7.26, 4.79 ppm ; 13C NMR δ [$CDCl_3$]: 77.0, ppm.

Synthesis Procedures (NMR characterization follows in Discussion of Results)

1-Allylimidazolium chloride (1-All-Im Cl): 1-allylimidazole (2 mL, 18.5 mmol) was added into a Schlenk flask, followed by 20 mL of hexane. After chilling to 0 °C with an ice bath, 1N HCl in Et_2O (23.0 mL, 23.0 mmol) was added drop wise with a syringe through a septum under nitrogen purge. The reaction was left to stir at RT overnight, with removal of the solvent yielding a white powder product (2.70 g, 18.68 mmol, 94.1% yield).

1-Allyl-3-Methylimidazolium iodide (1-All-3-Me-Im I): 1-allylimidazole (5.6 mL, 50 mmol) was added into a Schlenk flask, followed by 100 mL of toluene. After chilling to 0 °C with an ice bath, methyl iodide (3.8 mL, 61 mmol) was added drop wise with a syringe through a septum under nitrogen purge. After addition of MeI, the reaction mixture was allowed to stir at RT for 3 days. The solvent was removed on a vacuum line to dry the product, yielding a pale yellow powder (11.80g, 47.18 mmol, 94.3% yield).

1-Allyl-3-Benzylimidazolium chloride (1-All-3-Bz-Im Cl): 1-allylimidazole (5.0 mL, 46.2 mmol) was added into a Schlenk flask, followed by 50 mL toluene. After chilling to 0 °C with an ice bath, benzyl chloride (6.4 mL, 56.0 mmol) was added drop wise with a syringe through a septum under nitrogen purge. The reaction mixture was left to stir overnight at 80 °C in an oil bath. Removal of the solvent yielded a thick, viscous, brown liquid (8.40 g, 35.79 mmol, 77.4% yield).

Dichloromethylsilylpropylbenzene (DCMSPB, Karstedt): Allylbenzene (0.764 g, 6.47 mmol) was transferred into a Schlenk flask. A 0.1543 M solution of Karstedt's catalyst in toluene (0.10 mL, 0.24 mol %) was then injected through a septum into the solution while stirring under N_2 flow. This was followed by an injection of dichloromethylsilane, $HSiMeCl_2$ (1.0 mL, 9.70 mmol) and the mixture was allowed to stir overnight at RT. The resulting product was a dark purple-red liquid (1.868 g, yield not determined.)

Dichloromethylsilylpropylbenzene (DCMSPB, Pt(cod)Cl_2): $Pt(cod)Cl_2$ (20 mg, 1 mol %) was added into a Schlenk flask. Allylbenzene (0.764 g, 6.47 mmol) was then injected through a septum into the solution while stirring under N_2 flow. This was followed by an injection of dichloromethylsilane, $HSiMeCl_2$ (1.0 mL, 9.70 mmol) and the mixture was allowed to stir overnight at RT. The resulting product was a dark purple-red liquid (1.323 g, 87.7 % yield.)

1-Dichloromethylsilylpropyl-3-benzyl-imidazolium chloride (1-DCMSP-3-Bz-Im Cl): 1-All-3-Bz-Im Cl (2.46 g, 10.35 mmol) and $Pt(cod)Cl_2$ (20 mg, 0.053 mmol) were added to a Schlenk flask with a stirbar. Methylene chloride, CH_2Cl_2, was vapor transferred into the flask and was followed by injection of $HSiMeCl_2$ (1.35 mL, 1.25 mol equivalents) at room temperature over two minutes time. The resulting solution was left to stir overnight at RT, and removal of volatiles yielded a thick yellow-brown oil (2.94 g, 90.5 % yield).

1-Dichloromethylsilylpropyl-3-methyl-imidazolium iodide (1-DCMSP-3-Me-Im I): 1-All-3-Me-Im I (2.00 g, 8.00 mmol) and $Pt(cod)Cl_2$ (20 mg, 0.053 mmol) were added to a Schlenk flask with a stirbar. Methylene chloride, CH_2Cl_2, was vapor transferred into the flask and was followed by injection of $HSiMeCl_2$ (1.05 mL, 1.25 mol equivalents) at room temperature over two minutes time. The resulting

solution was left to stir overnight at RT, and removal of volatiles yielded a thick yellow-brown oil (1.79 g, 67.8 % yield).

1-Dichloromethylsilylpropylimidazolium chloride (1-DCMSP-Im Cl): 1-All-Im Cl (2.00 g, 13.83 mmol) and Pt(cod)Cl_2 (21 mg, 0.056 mmol) were added to a Schlenk flask with a stirbar. Methylene chloride, CH_2Cl_2, was vapor transferred into the flask and was followed by injection of $HSiMeCl_2$ (1.80 mL, 1.25 mol equivalents) at room temperature over two minutes time. The resulting solution was left to stir overnight at RT, and removal of volatiles yielded a viscous light brown liquid (2.84 g, 72.4 % yield).

1-Chlorodimethylsilylpropylimidazolium chloride (1-CDMSP-Im Cl): 1-All-Im Cl (2.00 g, 13.83 mmol) and Pt(cod)Cl_2 (21 mg, 0.056 mmol) were added to a Schlenk flask with a stirbar. Methylene chloride, CH_2Cl_2, was vapor transferred into the flask and was followed by injection of $HSiMe_2Cl$ (1.90 mL, 1.25 mol equivalents) at room temperature over two minutes time. The resulting solution was left to stir overnight at RT, and removal of volatiles yielded a transparent brown liquid (1.73g, 58.8 % yield).

1-Chlorodimethylsilylpropyl-3-benzylimidazolium chloride (1-CDMSP-3-Bz-Im Cl): 1-All-3-Bz-Im Cl (2.50 g, 10.52 mmol) and Pt(cod)Cl_2 (22 mg, 0.059 mmol) were added to a Schlenk flask with a stirbar. Methylene chloride, CH_2Cl_2, was vapor transferred into the flask and was followed by injection of $HSiMe_2Cl$ (1.46 mL, 1.25 mol equivalents) at room temperature over two minutes time. The resulting solution was left to stir overnight at RT, and removal of volatiles yielded a yellow-brown oil (1.86g, 60.2 % yield).

Sulfonation of 1-DCMSP-3-Bz-Im Cl: 1-DCMSP-3-Bz-Im Cl (1.40 g, 4.45 mmol) was added into a Schlenk flask. Methylene chloride, CH_2Cl_2, was vapor transferred into the flask, which was then taken into the glove box. Chlorosulfonic acid, $ClSO_3H$, (0.545 g, 4.68 mmol) was added into the flask via pipette, and instantaneous bubbling was observed. The resulting mixture was allowed to stir at room temperature overnight. Removal of volatiles yielded a yellow-brown oil (yield not measured).

Sulfonation of Benzyltrichlorosilane ($BzSiCl_3$): Benzyltrichlorosilane (0.500 g, 2.23 mmol) was added into a Schlenk flask. Methylene chloride, CH_2Cl_2, was vapor transferred into the flask, which was then pumped into the glove box. Chlorosulfonic acid, $ClSO_3H$, (0.286 g, 2.45 mmol) was added into the flask via pipette, causing the transparent solution to become cloudy and manifest an off-white hue. The resulting mixture was allowed to stir at room temperature overnight. Removal of volatiles yielded an off-white powder (yield not measured).

Synthesis for Dehydrated Trimethyltin Cube, ($(Si_8O_{20})(Me_3SnO)_8$): The cubic octaanion ((Si_8O_{20}) $(Me_4N)_8$) was prepared by dropwise addition of 1.1 eq of ultra-pure H2O into a stirring mixture of $Si(OEt)_4$ (tetraethylorthosilicate, TEOS, 1 eq) and 25 wt% Me_4NOH in methanol (tetramethylammonium hydroxide, 10 eq) in a plastic bottle at room temperature (RT) over 30 minutes. The bottle was then closed and stirred at RT for 18 hours.

The resulting solution was filtered to remove any undissolved material, transferred to an addition funnel and diluted with 20 mL of MeOH. The above solution was added dropwise over 7-10 hours to a vigorously stirred, cooled solution (0 °C) of Me_3SnCl (trimethyltin chloride, 1.2 eq) in ~200mL of Et_2O

under a slow nitrogen purge. The cloudy white solution was stirred overnight and allowed to return to room temperature.

The solution was then placed into a separatory funnel and the organic phase was separated from the milky white aqueous phase. If clear phase separation did not occur, diethylether (Et_2O) was added in 5 mL aliquots until two phases were apparent. The aqueous phase was extracted three times with ~75mL aliquots of Et_2O. The combined organic phase was dried over anhydrous $MgSO_4$ (magnesium sulfate, ~15g) for 2 hours. Upon filtration, the solvent was removed under vacuum until a dry white residue formed.

The residue was refluxed in ~400mL of toluene in air until it dissolved. If complete dissolution did not occur, then the hot solution was filtered after which the toluene was removed and the sample dried under vacuum at RT. The white product residue was then redissolved in refluxing hexanes (~300mL) in air, which was reduced to ~30mL for recrystallization. If the hot hexanes solution remained cloudy, then a hot filtration was carried out before solvent volume reduction. The reduced solution was slowly cooled to room temperature at which point colorless needle like crystals began to form. Once the solution reached room temperature the solution was cooled to 5 °C overnight. The mother liquor was decanted from the crystals which were then dried under vacuum. Recrystallized yield for a 20mL (TEOS) scale is generally 15-18g of $((Si_8O_{20})(Me_3SnO)_8)$ for ~70 - 90% yield. The crystals were ground into a fine powder and dried under vacuum at 100 °C overnight to ensure removal of any waters of hydration.

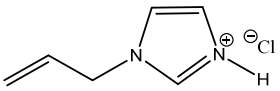

1-Allylimidazolium chloride
(1-All-Im Cl)

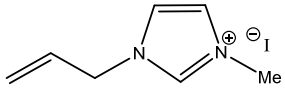

1-Allyl-3-Methylimidazolium iodide
(1-All-3-Im I)

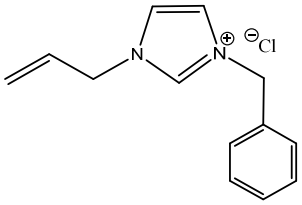

1-Allyl-3-Benzylimidazolium chloride
(1-All-3-Bz-Im Cl)

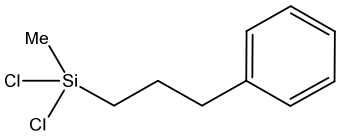

Dichloromethylsilylpropylbenzene
(DCMSPB)

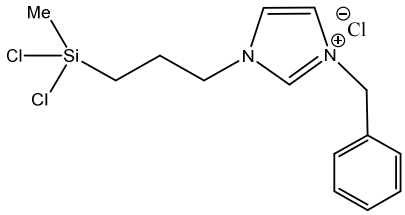

1-Dichloromethylsilylpropyl-3-Benzylimidazolium chloride
(1-DCMSP-3-Bz-Im Cl)

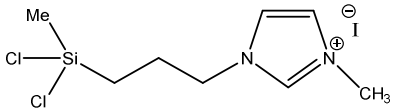

1-Dichloromethylsilylpropyl-3-Methylimidazolium iodide
(1-DCMSP-3-Me-Im I)

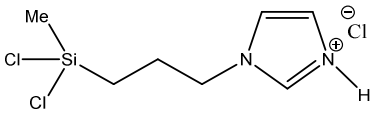

1-Dichloromethylsilylpropylimidazolium chloride
(DCMSP-Im Cl)

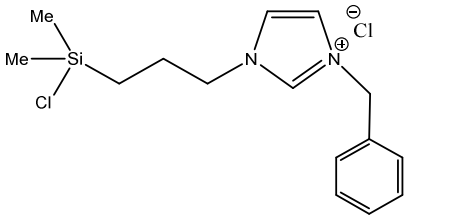

1-Chlorodimethylsilylpropyl-3-Benzylimidazolium chloride
(1-CDMSP-3-Bz-Im Cl)

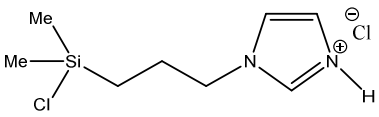

1-Chlorodimethylsilylpropylimidazolium chloride
(1-CDMSP-Im Cl)

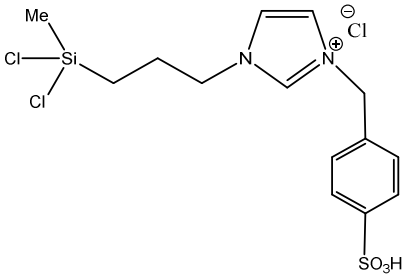

1-Dichloromethylsilylpropyl-3-benzyl sulfonic acid-imidazolium chloride
(1-DCMSP-3-BSA-Im Cl)

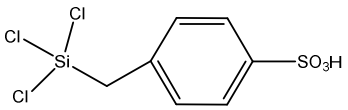

1-Sulfonic acid-4-trichloromethylsilylbenzene
(1-SA-4-TCMSB)

Figure 20: Synthesized Compounds and their Abbreviations

Part 2: Synthesis of Ionic Liquid Linking Agents

Three major ionic liquid variants stemming from 1-allylimidazole were synthesized in the intial phase of this research. This includes 1-allylimidazolium chloride (1-All-Im Cl), 1-allyl-3-Methylimidazolium iodide (1-All-3-Me-Im I), and 1-allyl-3-Benzylimidazolium chloride (1-All-3-Bz-Im Cl). The synthetic procedures are described in the experimental section, with ^{1}H NMR spectra characterizing the products shown below (see Figure 20 above for interpretation of abbreviations):

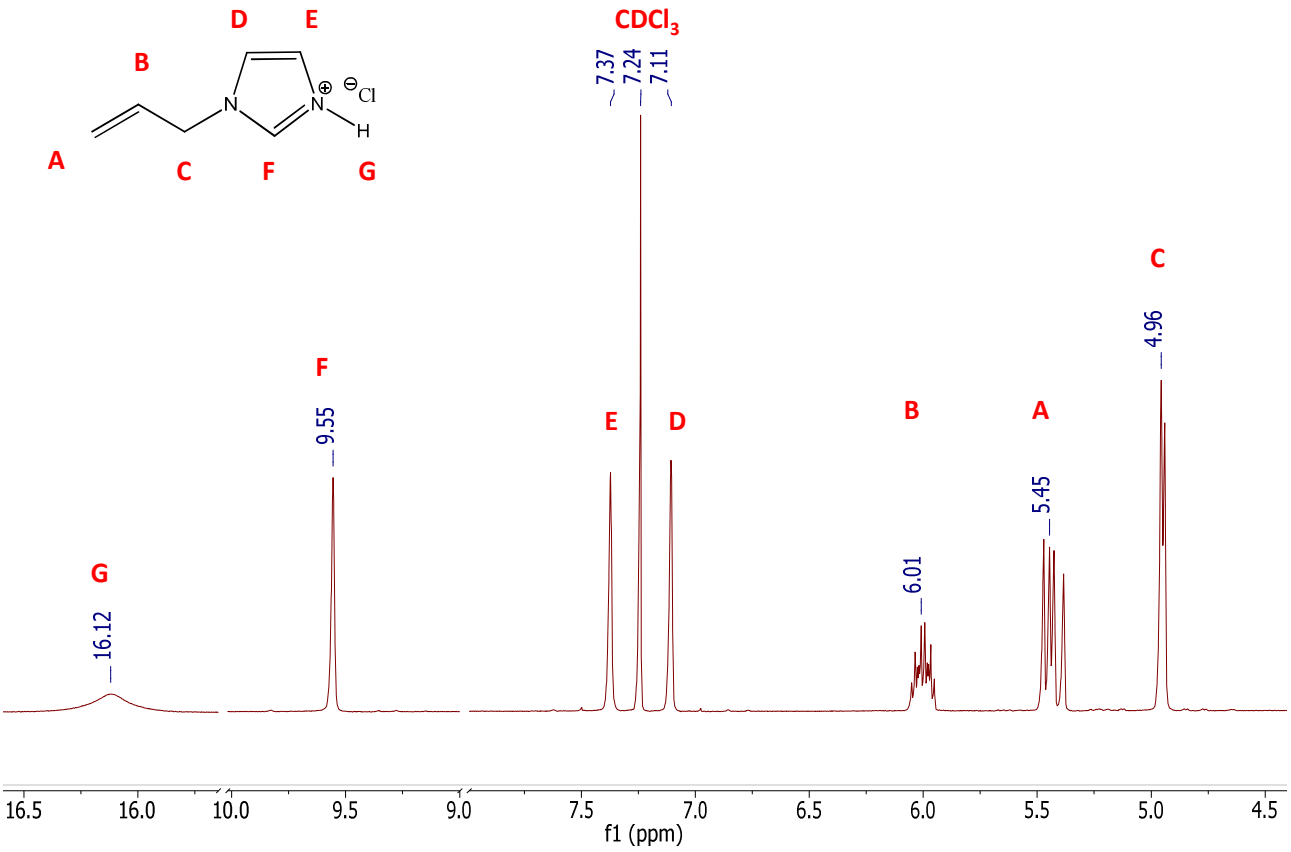

Figure 21: ^{1}H NMR spectrum of 1-All-Im Cl (400 MHz, $CDCl_3$, 23 °C)

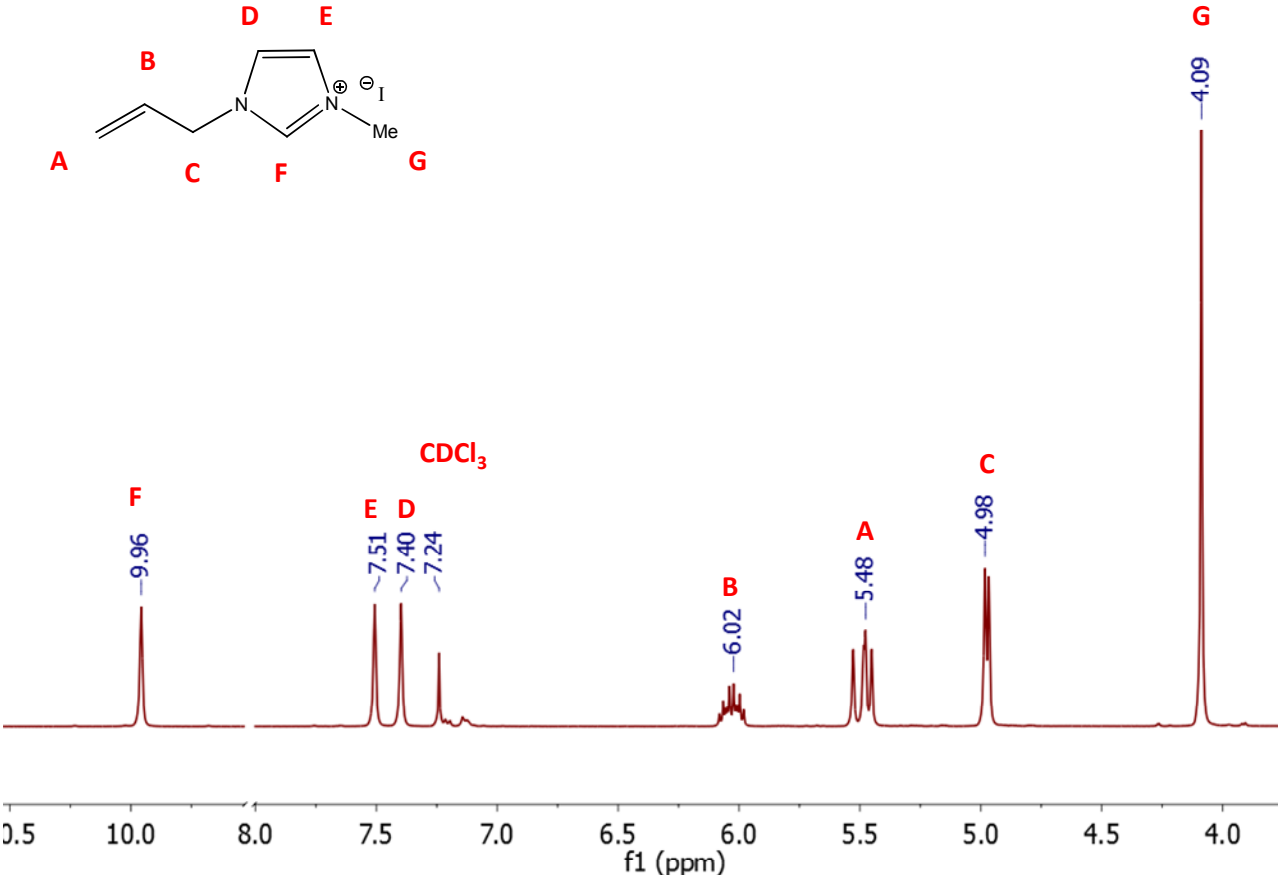

Figure 22: ^{1}H NMR spectrum of 1-All-3-Me-Im I (400 MHz, $CDCl_3$, 23 °C)

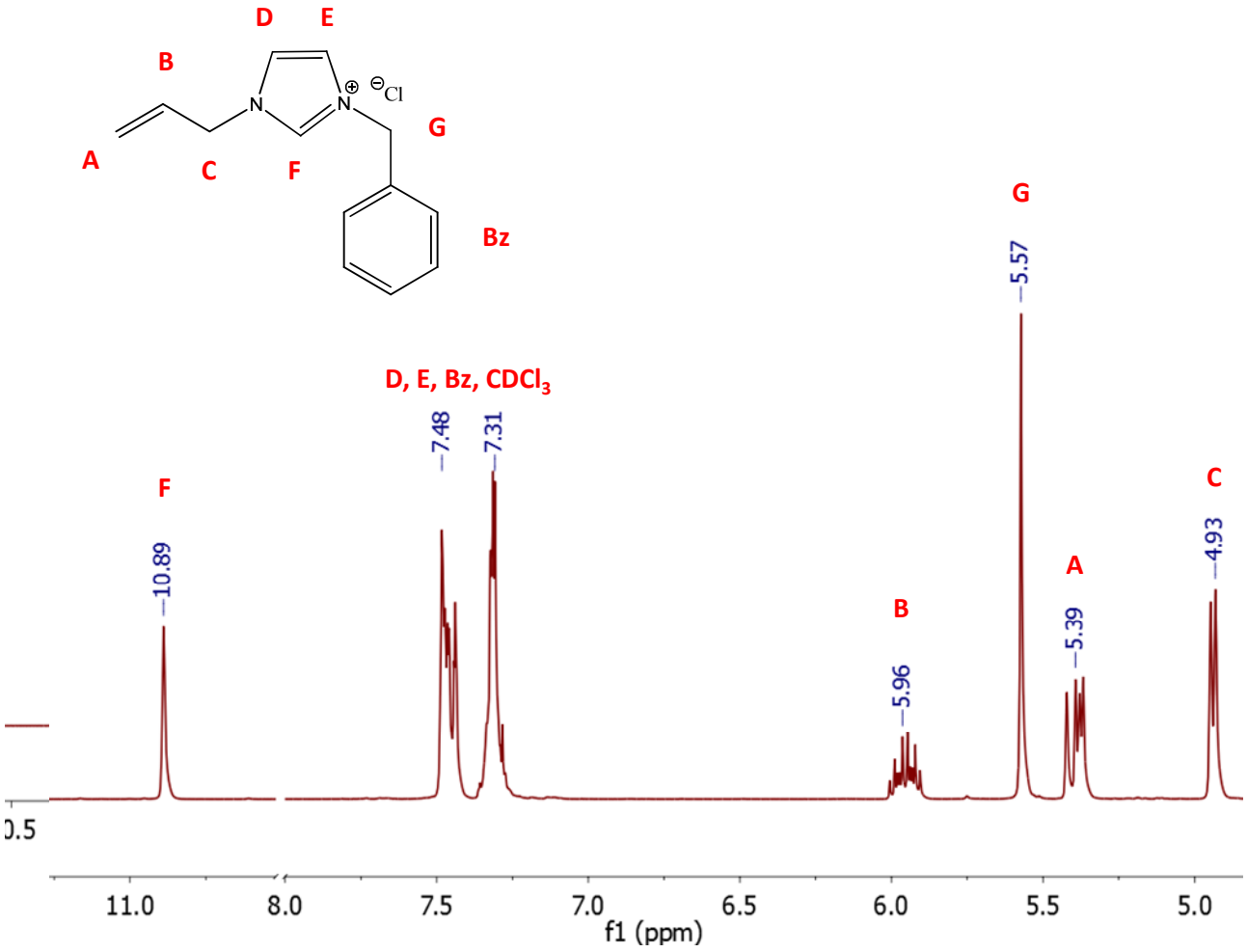

Figure 23: ^{1}H NMR spectrum of 1-All-3-Bz-Im Cl (400 MHz, $CDCl_3$, 23 °C)

Protonation or N-alkylation of allylimidazole was a straightforward reaction with high yields for all reagents tested. Next, a hydrosilation reaction was necessary to create the chlorosilane functionality required for a linking reaction between the cube and these ionic liquids. Initial hydrosilation reaction attempts with Karstedt's catalyst proved unsuccessful, so allylbenzene was substituted for the ionic liquid reactants as a model to determine the best set of reaction conditions. Of particular interest was the platinum catalyst used, as well as the silane varieties that could be successfully employed.

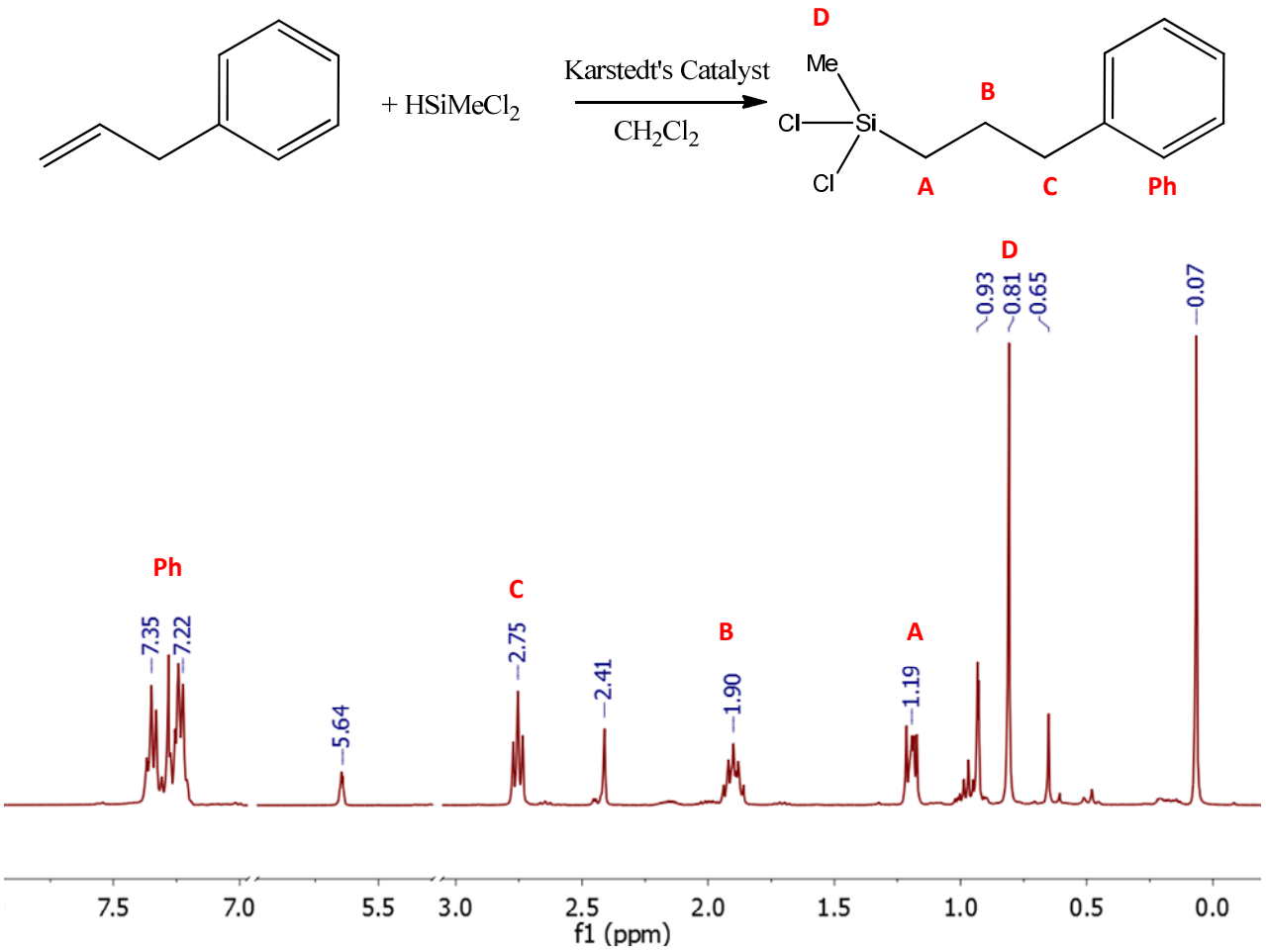

Figure 24: ^{1}H NMR spectrum of DCMSPB via Karstedt's catalyst(400 MHz, $CDCl_3$, 23 °C)

As shown in Figure **24** above, the reaction product using Karstedt's catalyst is impure. While peaks were identified that were consistent with the presence of the expected product, there are additional resonances that cannot be attributed to either of the starting materials suggesting that multiple reaction products were formed. For comparison, the previous reaction was then repeated, substituting dichlororo(1,5-cyclooctadiene)platinum (II), $Pt(cod)Cl_2$ in for Karstedt's catalyst:

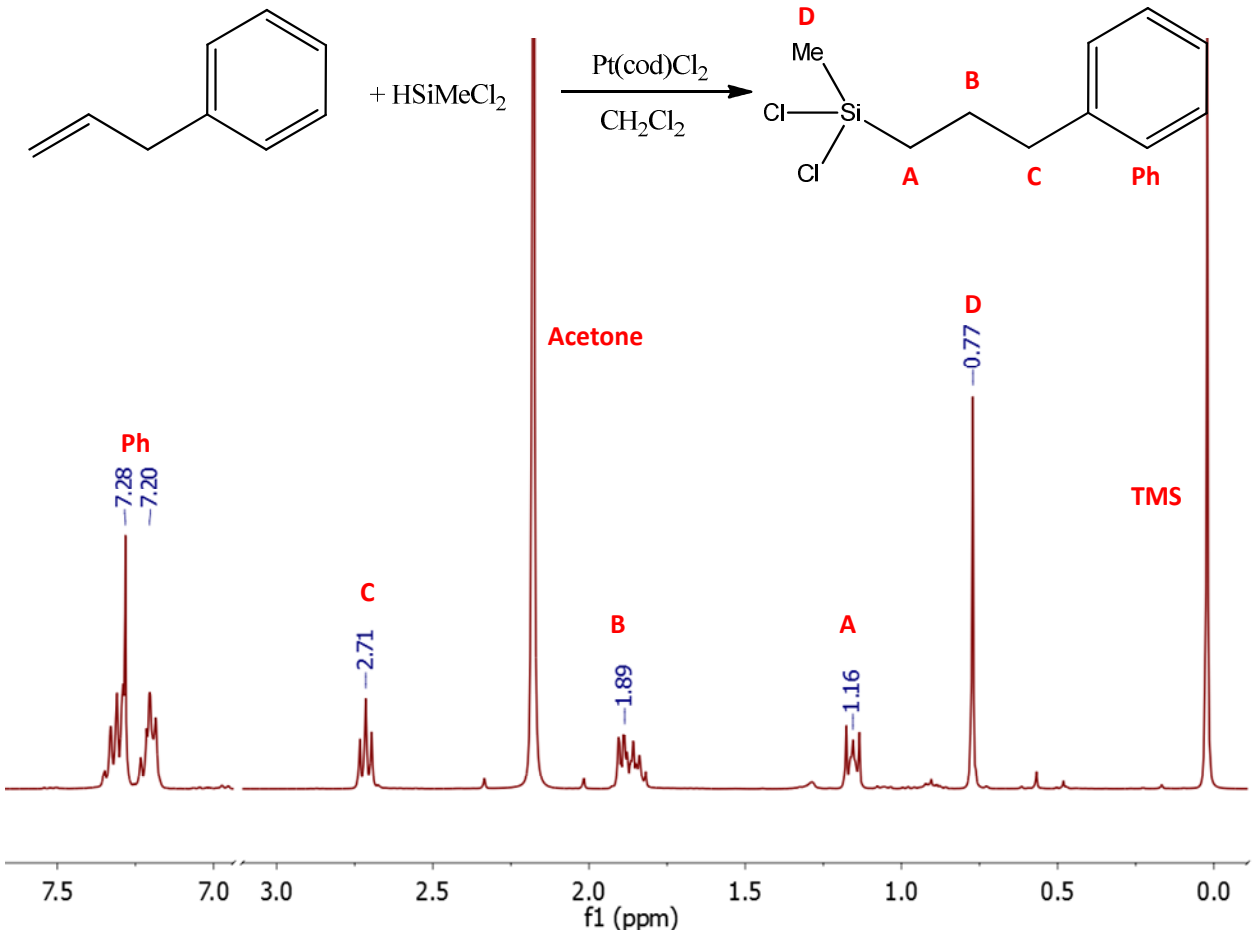

Figure 25: ^{1}H NMR spectrum of DCMSPB via Pt(cod)Cl$_2$ (400 MHz, CDCl$_3$, 23 °C)

Figure 25 reveals that the expected product has been formed. These analogous reactions suggest that the desired hydrosilated product synthesized utilizing Pt(cod)Cl$_2$ contains fewer impurities than the products that form in the presence of Karstedt's catalyst.

It would be beneficial to be able to complete the hydrosilation with a variety of different silane linkers in order to have more control over the connectivity of the final product. Previous work by postdoctoral investigator Jim Chen showed that hydrosilation reactions employing HSiCl$_3$ were more difficult to effect in terms of product yield and purity than reactions with HSiMeCl$_2$, however curiosity still remained as to the effectiveness of HSiMe$_2$Cl. This reaction was also attempted with the model allylbenzene system, with a ^{1}H spectrum of the resulting product shown in Figure 26 below.

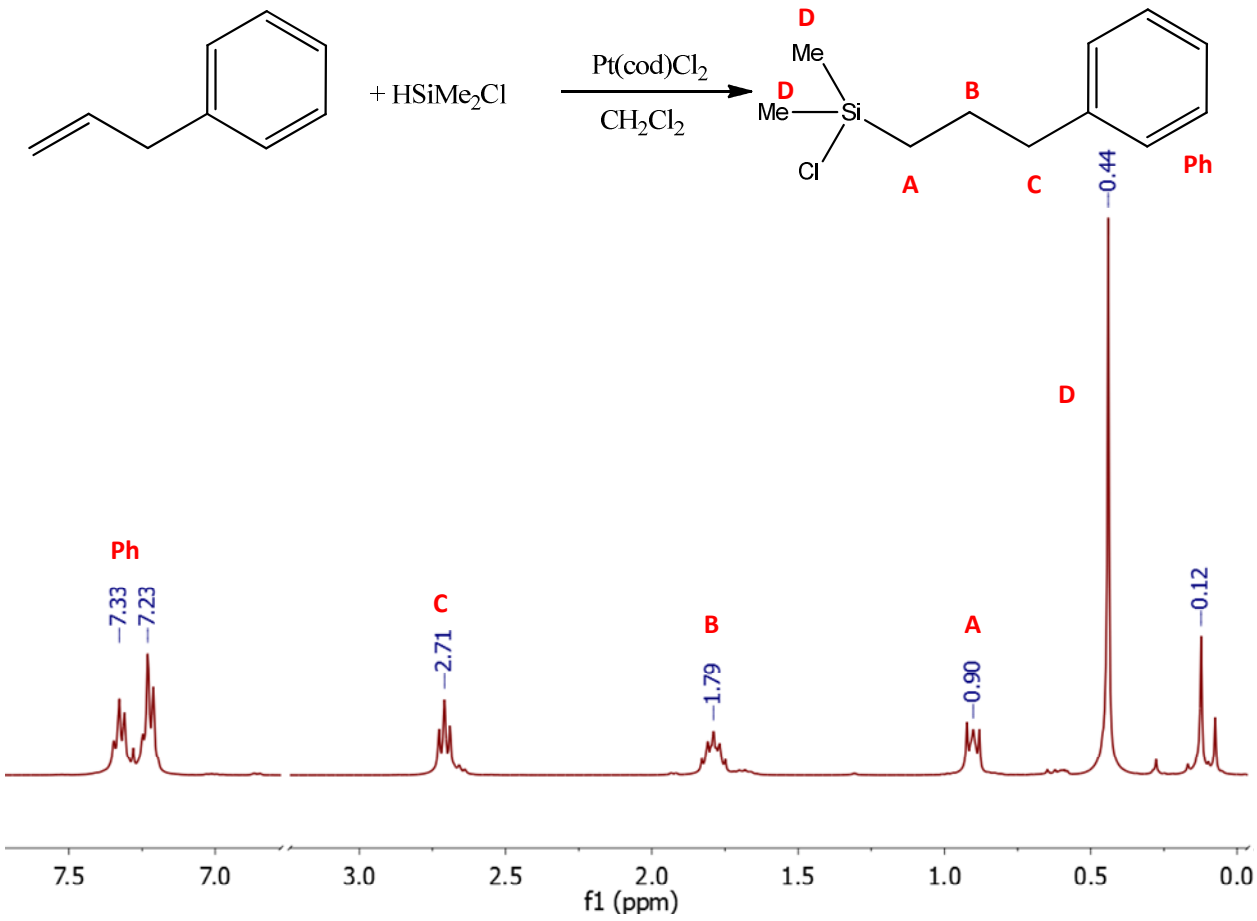

Figure 26: ^{1}H NMR spectrum of DMCSPB via Pt(cod)Cl$_2$ (400 MHz, CDCl$_3$, 23 °C)

The spectrum in Figure 26 matches the expected signature for the desired product, supporting the notion that the hydrosilation reaction will allow for flexibility in the silane that is added onto the linking agent. At this point, it was felt that a basic understanding of the hydrosilation reaction had been developed, so the decision to return to hydrosilation of ionic liquids was made.

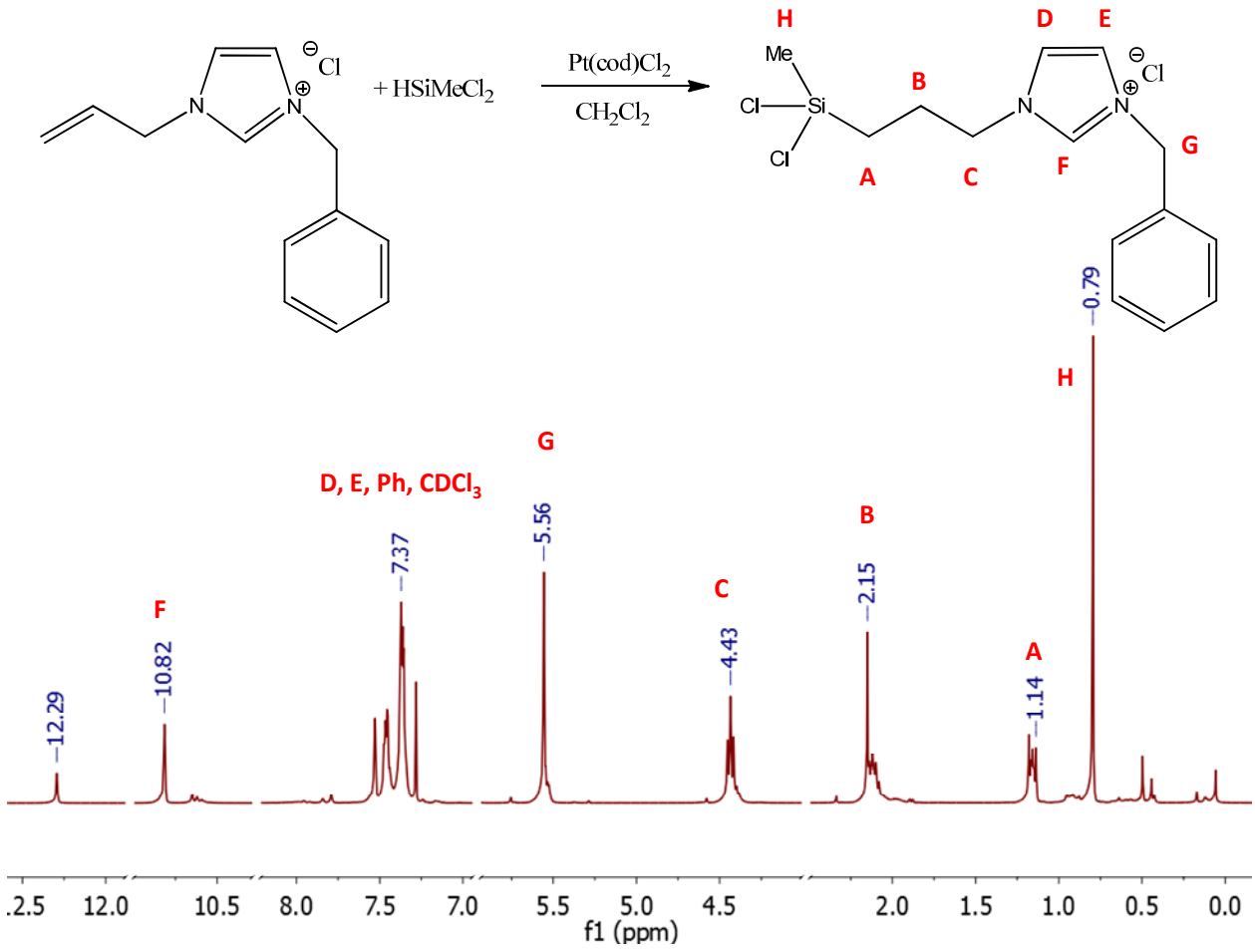

Figure 27: ^{1}H NMR spectrum of 1-DCMSP-3-Bz-Im Cl (400 MHz, $CDCl_3$, 23 °C)

Figure 27 shows the spectrum of the product mixture from the hydrosilation of 1-All-3-Bz-Im Cl with $HSiMeCl_2$. The observed signals correlate well with the spectrum of the expected product, with the exception of an unknown peak far upfield at ~12.3 ppm. This reaction was repeated numerous times with various yields of the desired product, making it apparent that it does not possess a high degree of reproducibility. ^{1}H spectra occasionally showed a high percentage of starting material remaining, even when all reaction parameters were identical to previous attempts.

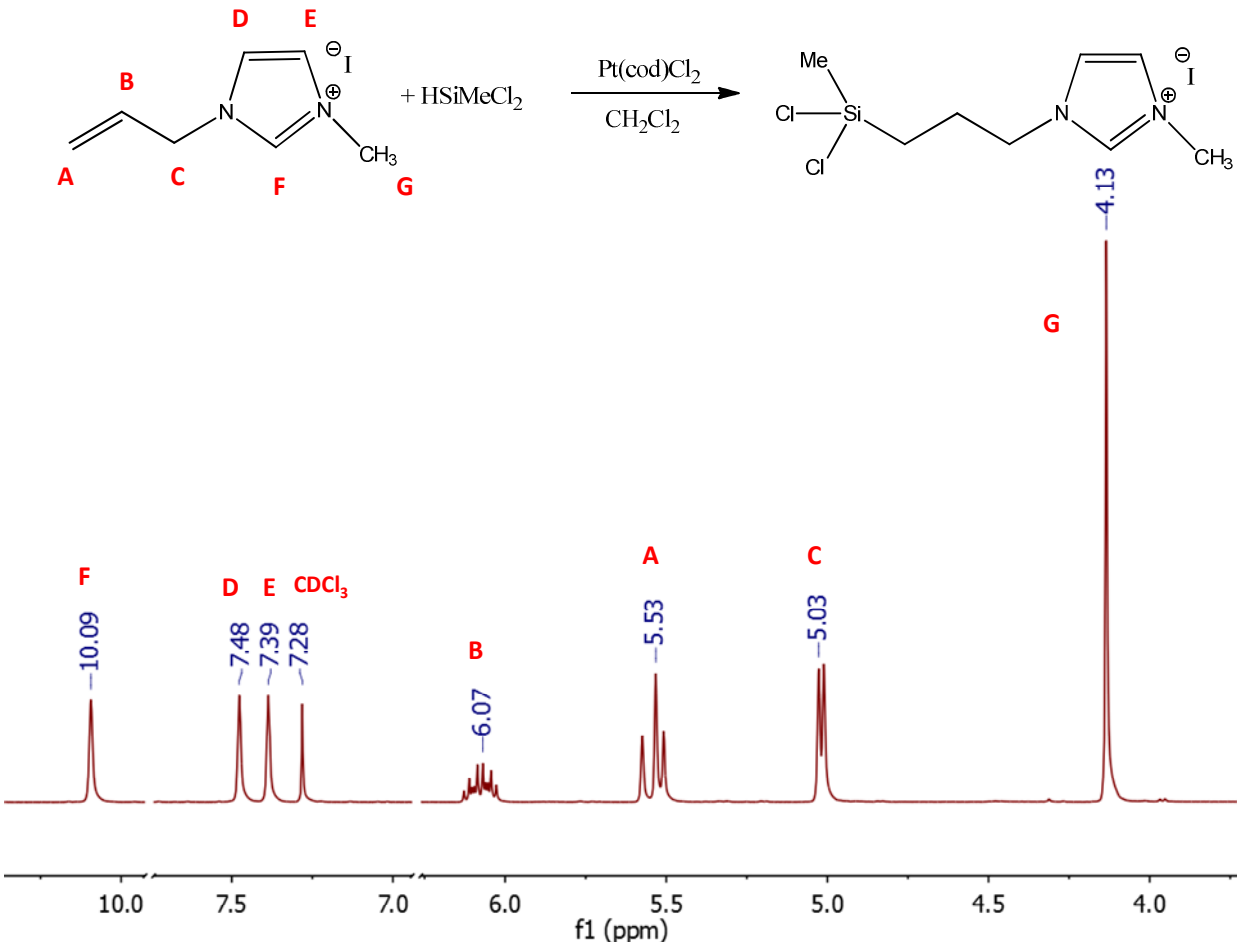

Figure 28: ^{1}H NMR spectrum of 1-DCMSP-3-Me-Im I (400 MHz, $CDCl_3$, 23 °C)

Figure 28 clearly shows that 1-All-3-Me-Im I was unaffected under these reaction parameters. The collected product is entirely 1-All-3-Me-Im I, with no trace of the desired product being formed.

Curious as to the failure of the hydrosilation reaction of 1-All-3-Me-Im I, addition methodology was considered as a possibility for failure of the reaction. Parallel hydrosilation reactions were set up with 1-All-Im Cl to examine differences between vapor diffusion and injection as the method for silane addition.

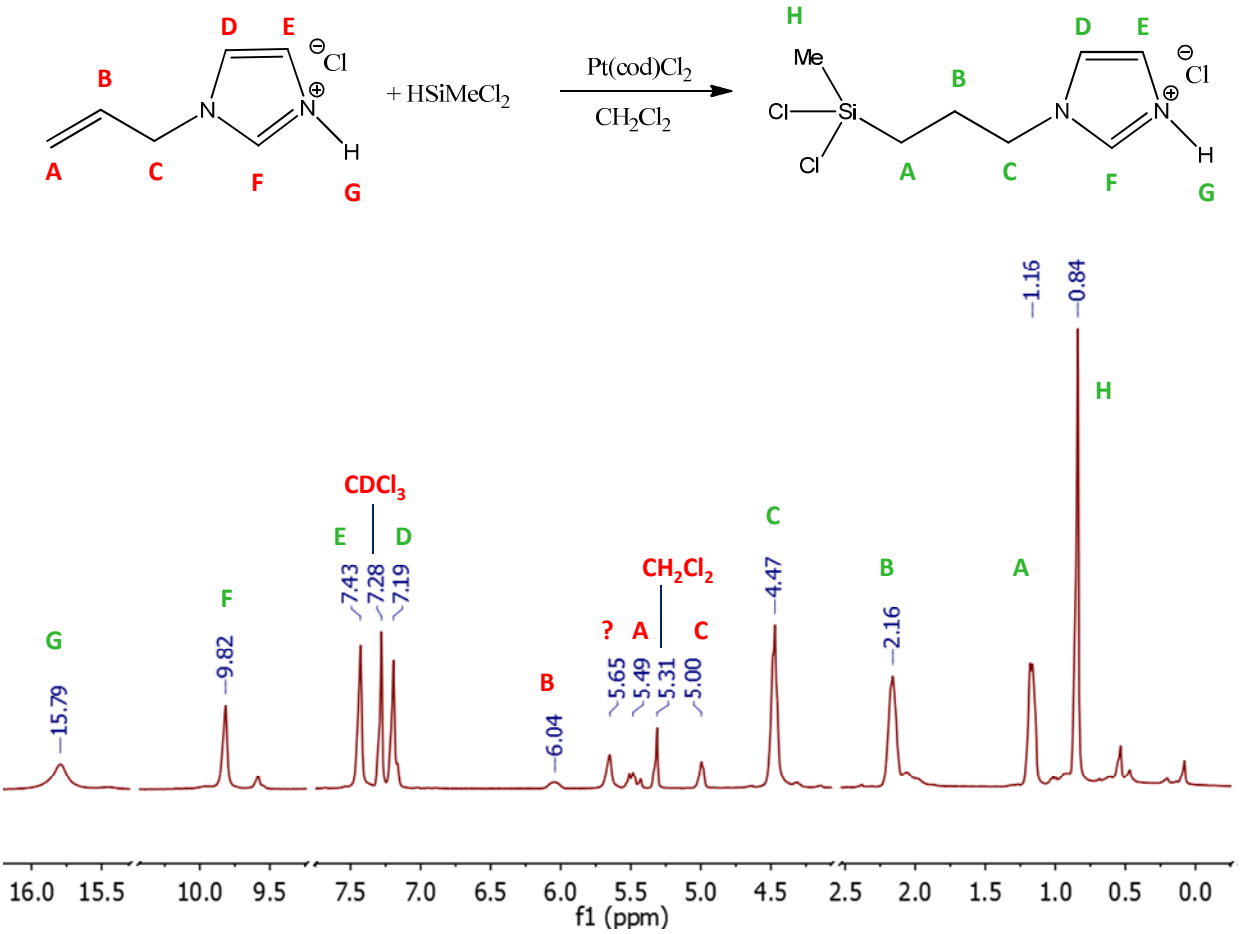

Figure 29: ^{1}H NMR spectrum of 1-DCMSP-Im Cl via diffusion (400 MHz, $CDCl_3$, 23 °C)

Figure 29, showing the spectrum for the diffusion product shows a mixture of starting materials and products, indicating incomplete conversion of the reactants. Assuming that the silane was present in sufficient excess to react with all of the 1-allyl-imidazolium chloride, this suggests that the reaction proceeds more slowly for diffusion than for when $HSiMeCl_2$ is injected.

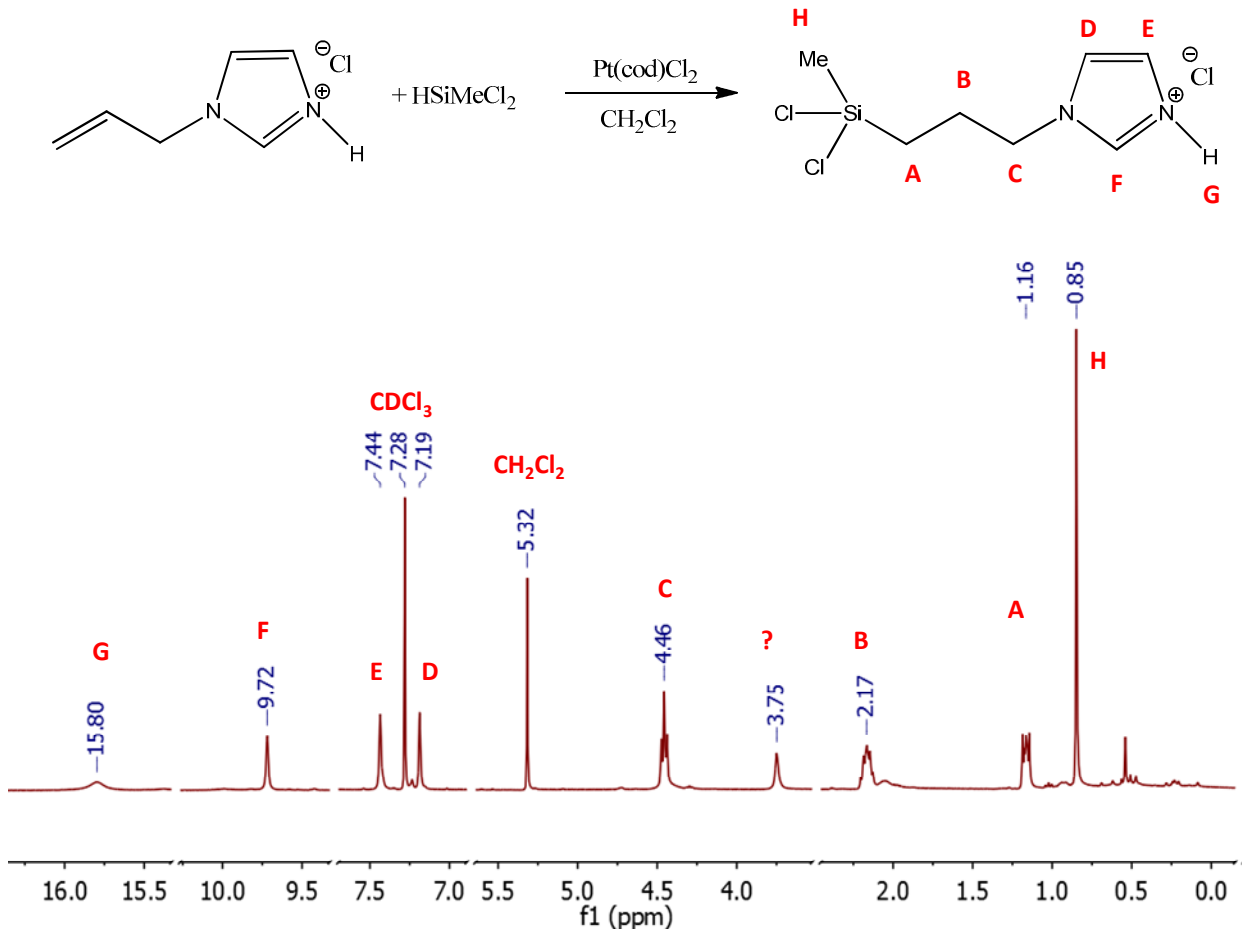

Figure 30: ^{1}H NMR spectrum of 1-DCMSP-Im Cl via injection (400 MHz, $CDCl_3$, 23 °C)

With the exception of an unknown peak appearing at σ = 3.75 ppm, the spectrum in Figure 30 shows formation of the expected product with no trace of starting material remaining. In combination with the results from the diffusion experiment, it appears that using injection as a silane addition technique is more effective in the conversion of starting materials to products in this hydrosilation reaction. From this point onwards, this conclusion was generalized to all other hydrosilation reactions. Additionally, the failure to convert 1-All-3-Me-Im I to 1-DCMSP-3-Me-Im I was assumed to indicate an unfavorable reaction. Although this may not be the case with increased temperature or pressures, for the ease of convenience all further experimentation was limited to 1-DCMSP-3-Bz-Im Cl and 1-DCMSP-Im Cl.

As previously mentioned, the capability to vary the silane utilized in the hydrosilation reaction would lead to a wider variety of products, allowing for a more precise design of the implemented catalyst. Thus, some testing was also carried out using chlorodimethylsilane, as documented in the pages that follow.

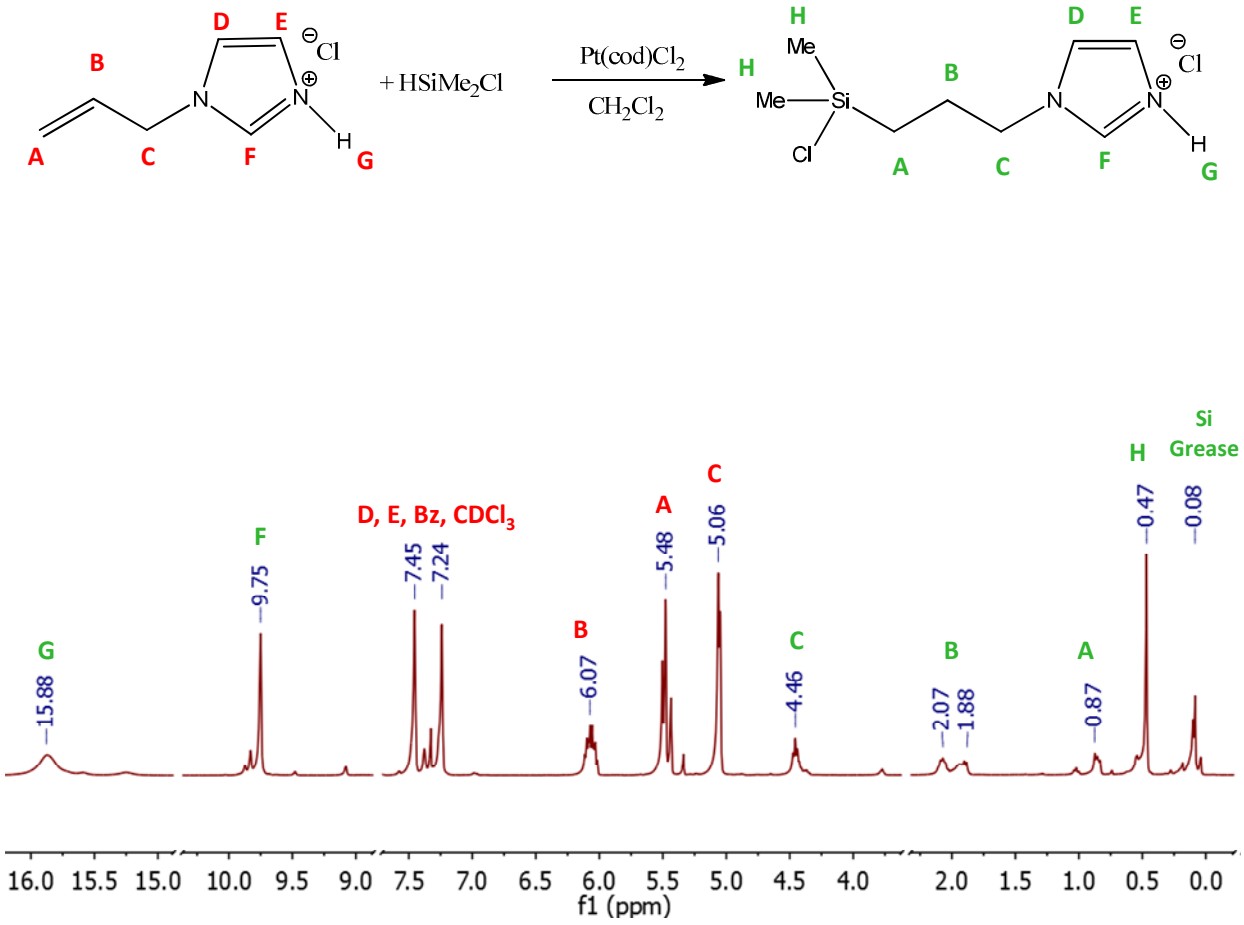

Figure 31: ^{1}H NMR spectrum of 1-CDMSP-Im Cl (400 MHz, $CDCl_3$, 23 °C)

The hydrosilation of 1-All-3-H-Im Cl with of $HSiMe_2Cl$ was attempted as just described. Figure 31 shows that a mix of reactants and products were isolated post reaction, indicating an incomplete reaction. Aside from this fact, there are not a large amount of contaminants or undesired reaction products, meaning it may be viable with altered reaction parameters, including time, temperature, or pressure.

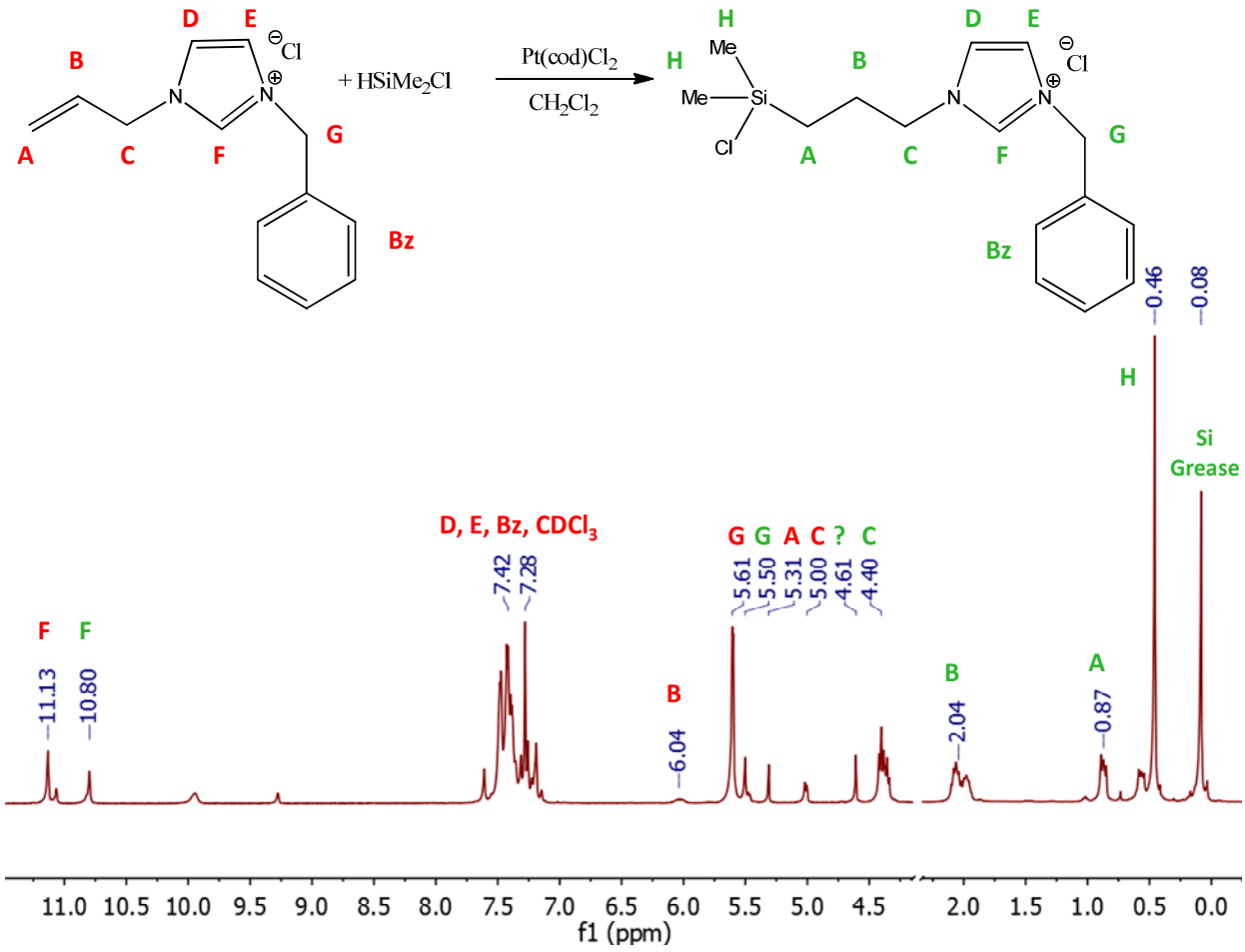

Figure 32: ^{1}H NMR spectrum of 1-CDMSP-3-Bz-Im Cl (400 MHz, $CDCl_3$, 23 °C)

Hydrosilation of 1-All-3-Bz-Im Cl with $HSiMe_2Cl$ behaves similarly to hydrosilation of 1-All-3-H-Im Cl. Although more difficult to interpret, Figure 32 shows peaks corresponding to a mixture of both reactants and products. Again, it may be possible to adjust reaction parameters to find a favorable set of conditions, however given the success of hydrosilation reactions with $HSiMeCl_2$, it was deemed to be a more effective use of time to proceed with those products. Thus, for the remaining stages of catalyst development, sulfonation and the linking reaction, the most promising candidates, 1-DCMSP-3-Bz-Im Cl and 1-DCMSP-Im Cl, were investigated exclusively.

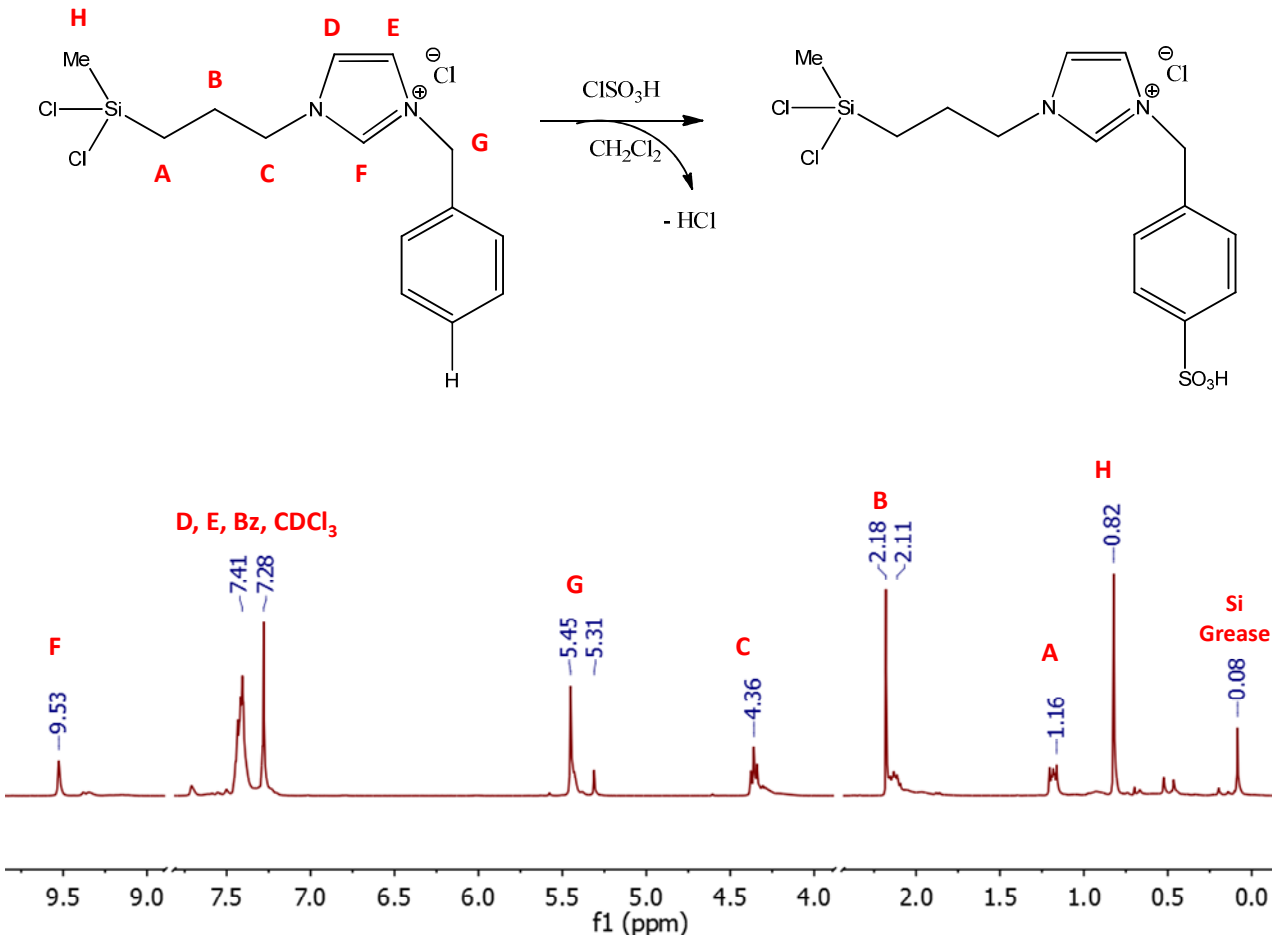

Figure 33: ^{1}H NMR spectrum for 1:1 sulfonation of 1-DCMSP-3-Bz-Im Cl (400 MHz, $CDCl_3$, 23 °C)

Once silylated, we attempted to create a bifunctional linker by sulfonating the aromatic ring of 1-DCMSP-3-Bz-Im Cl with $ClSO_3H$. Based on the absence of both a new upfield singlet and a doublet of doublets emerging in the aromatic region in Figure 33, signifying a conversion to the desired products, it appears as though only starting material was isolated from this reaction. However, considering that the absence of evidence is not a strong foundation on which to base a conclusion, additional solvent was added to these products, along with another mol equivalent of chlorosulfonic acid to attempt to elicit the desired sulfonated product.

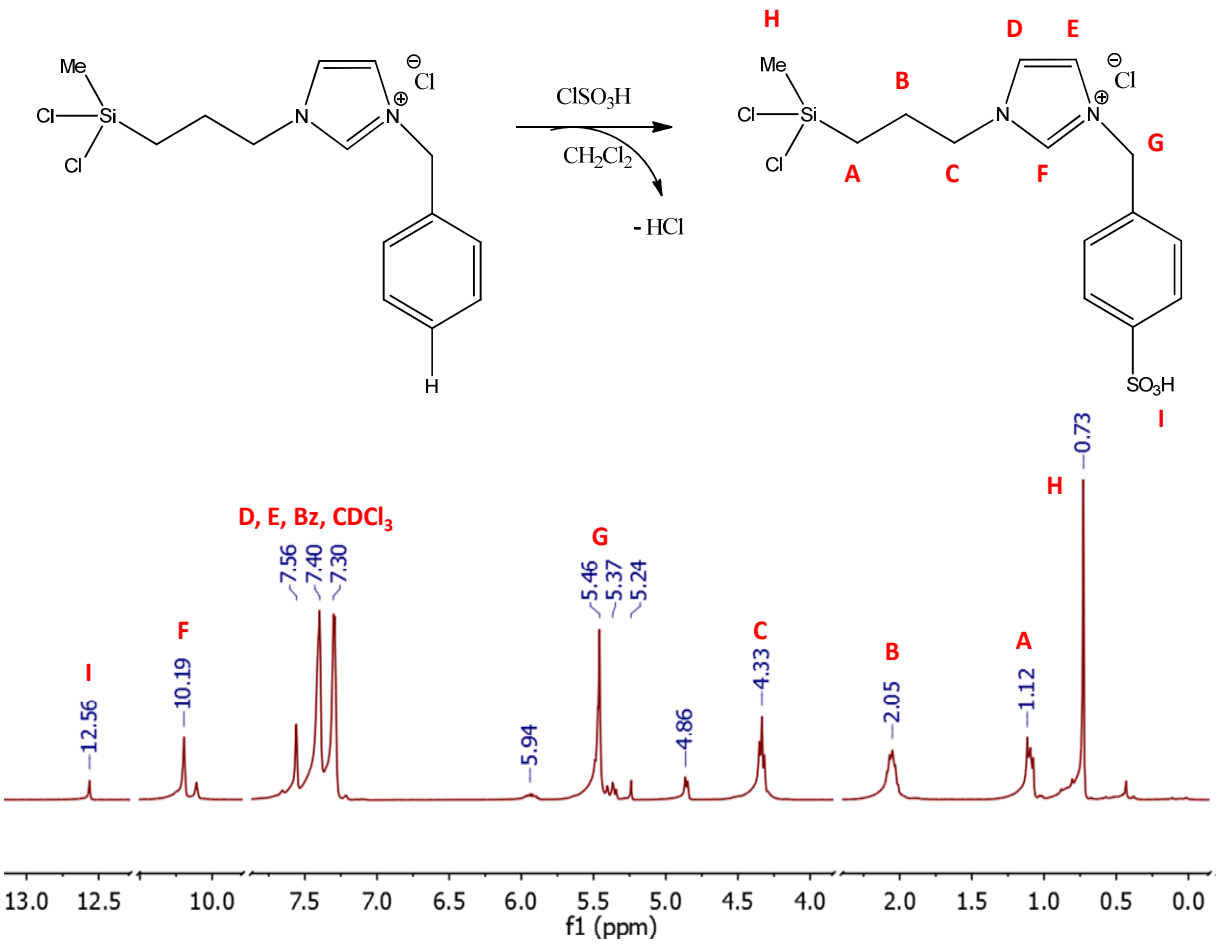

Figure 34: ^{1}H NMR spectrum for 2:1 sulfonation of 1-DCMSP-3-Bz-Im Cl (400 MHz, $CDCl_3$, 23 °C)

At a 2:1 ratio of chlorosulfonic acid to 1-DCMSP-3-Bz-Im Cl, it seems that the sulfonated product is beginning to form. This is indicated by the singlet forming at σ = 12.56 ppm, and the divergence of the peaks in the aromatic region into a doublet of doublets (σ = 7.30, 7.40 ppm). However, based on the relative area of the peaks, it appears as though the conversion is not yet complete. Thus, an uncalculated excess of chlorosulfonic acid was added as described in the previous reaction to bring the total ratio to be estimated between 4:1 and 8:1.

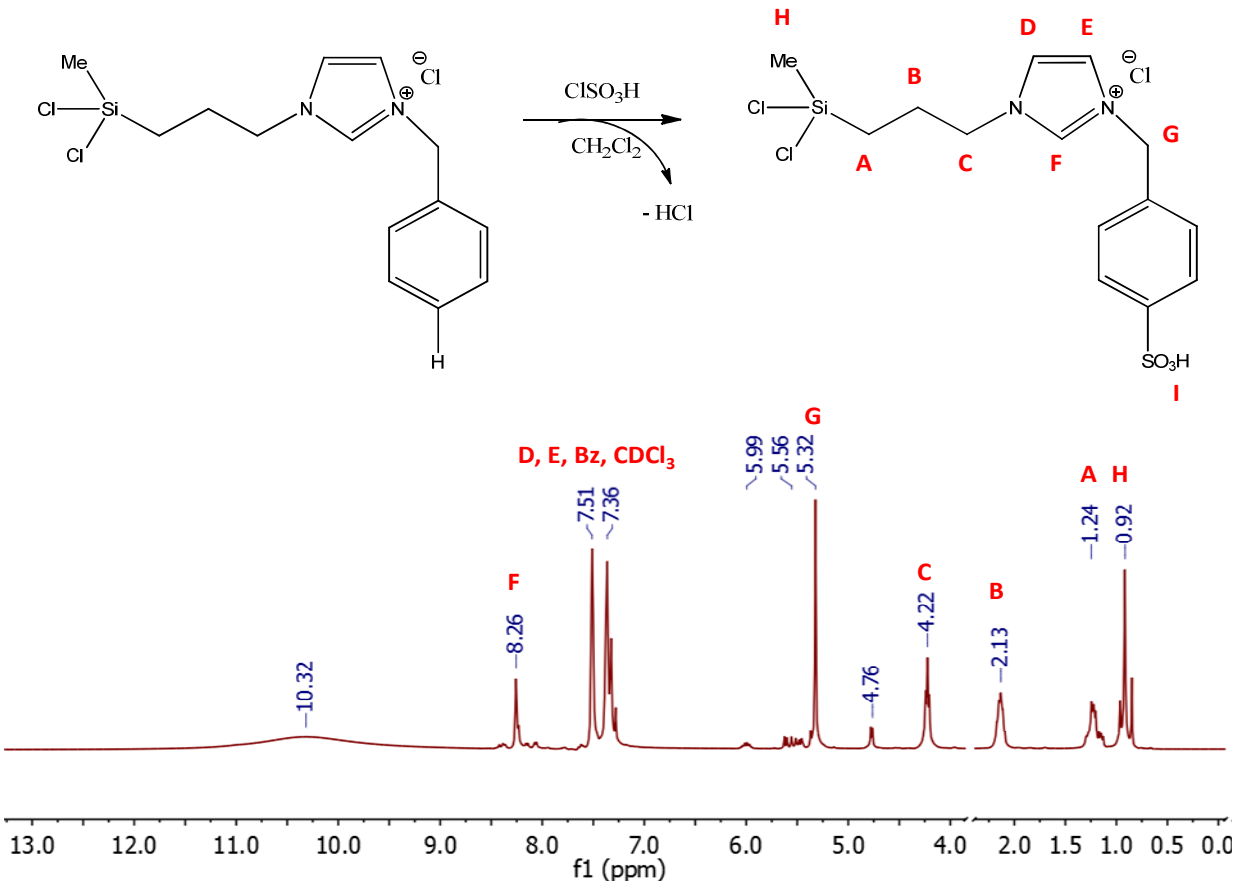

Figure 35: ^{1}H NMR spectrum of 1-DCMSP-3-Bz-Im Cl with excess $ClSO_3H$ (400 MHz, $CDCl_3$, 23 °C)

Reaction of 1-All-3-Bz-Im Cl with an excess of $ClSO_3H$ gives rise to a product mixture, the ^{1}H spectrum of which is shown in Figure 35. While the downfield peaks remain much unchanged, including trace signatures of the allyl protons from 1-All-3-Bz-Im Cl (σ = 4.76, 5.56, 5.99 ppm), the peaks upfield have shifted significantly, indicating a change has occurred near the more electron withdrawing imidazolium or benzyl ring. Given that the singlet from Figure 34, appearing at σ = 12.56 ppm, in which a controlled substitution had begun to occur has vanished and is replaced by a broad feature at σ = 10.32 ppm, it is suspected that the structure has been unintentionally damaged by the high reactivity of chlorosulfonic acid, rather than the possibility that excess acid remains in solution.

Having suspected at this point that there is some interference from the ionic functionality on the linking agent making it difficult to control the sulfonation reaction with precision, experimentation was shifted to a simpler linker that shares some commonalities, benzyltrichlorosilane ($BzSiCl_3$).

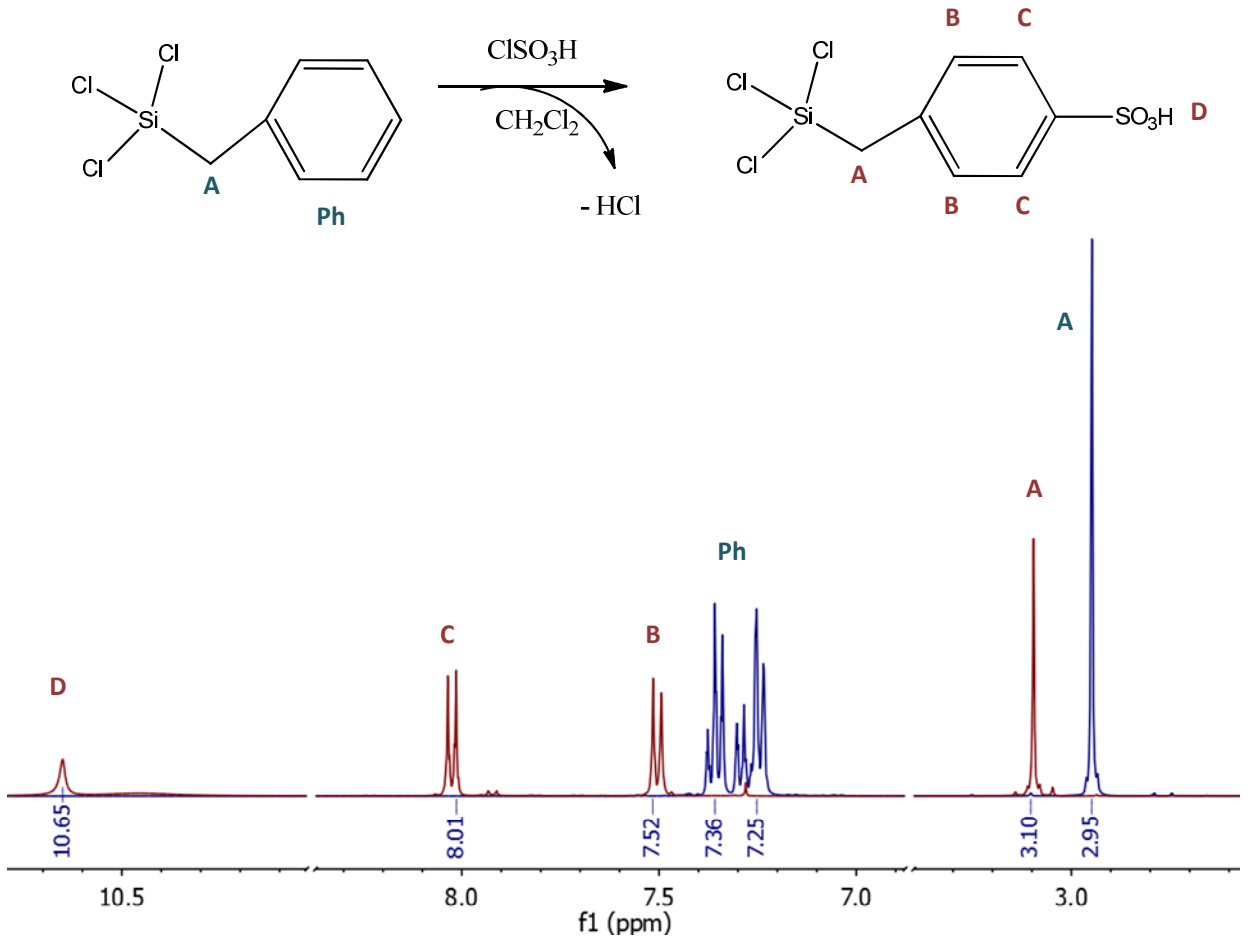

Figure 36: ^{1}H NMR spectrum of sulfonation of $BzSiCl_3$ (400 MHz, $CDCl_3$, 23 °C)

Figure 36 displays the reactant and products for the sulfonation of $BzSiCl_3$. The overlay very neatly displays the sulfonation reaction to convert $BzSiCl_3$ (blue, reactant) to HSO_3-$BzSiCl_3$ (red, product)as successful. This is most evident by the changes observed in the region between σ = 7.0 - 8.0 ppm. In the starting material, the ring protons are only slightly magnetically inequivalent, creating insufficient differences to completely resolve their resonance signatures. However, after para-substitution has fully occurred in the product, the remaining ring protons form two magnetically distinct sets. Each set splits the other into a doublet splitting pattern by the n+1 rule, yielding two sets of doublets. Furthermore, the chemical shift separation between these two sets is greatly increased in the product relative to the reactant as a result of the electron withdrawing properties of the sulfonic acid functionality to deshield those protons. In addition, the acidic functionality creates its own signature at σ = 10.65 ppm, leaving no doubt that this reaction proceeded in a controlled manner to completion.

This is supported by the upfield shift of peaks observed in the ^{13}C NMR spectra of $BzSiCl_3$ before and after exposure to chlorosulfonic acid, shown in Figures 37 and 38, below. Additionally, no changes were seen in the ^{29}Si spectra (not shown, single peak at σ = 5.91 ppm), suggesting that the Si–Cl bonds at the linking point were unaffected.

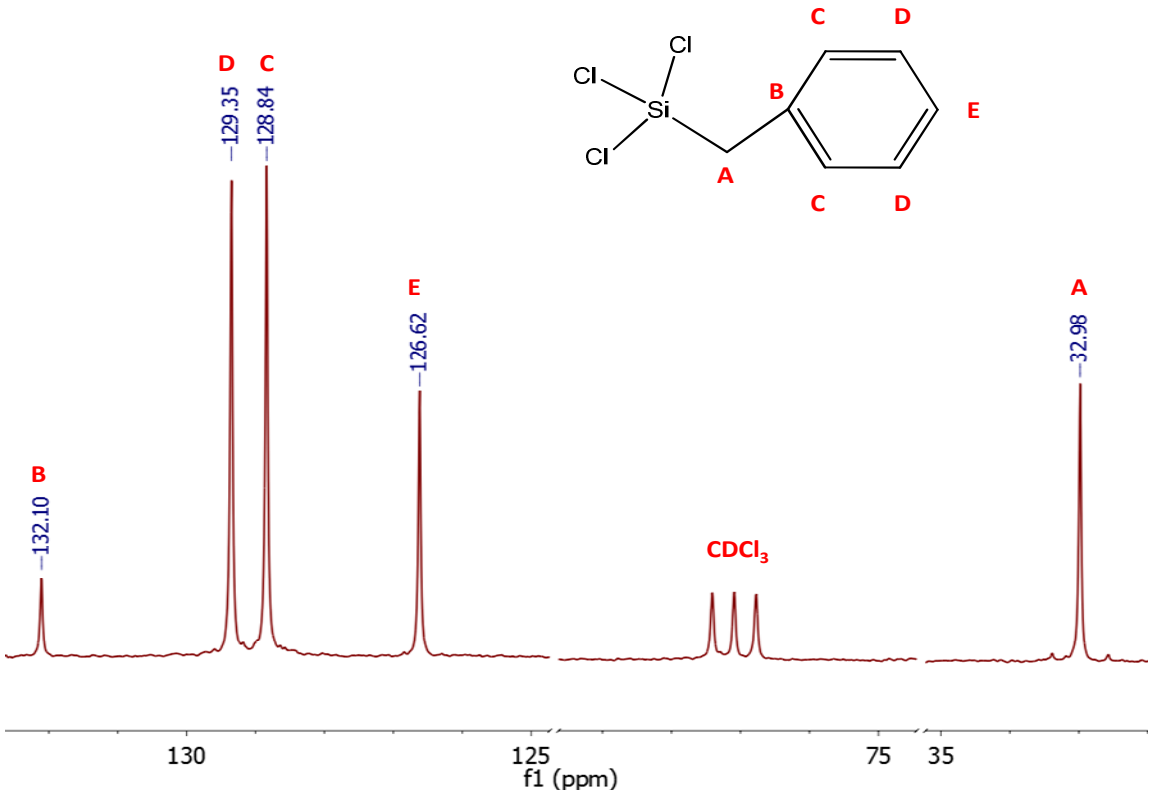

Figure 37: ^{13}C NMR spectrum of $BzSiCl_3$ pre-sulfonation (400 MHz, $CDCl_3$, 23 °C)

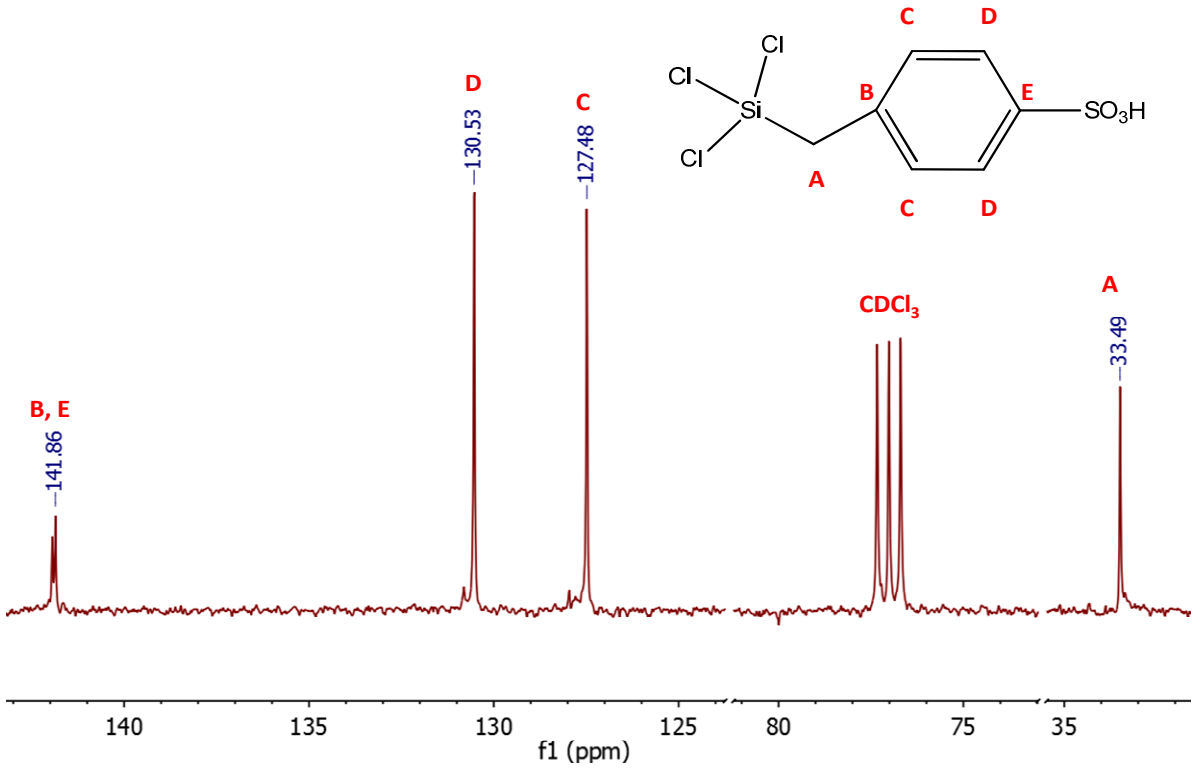

Figure 38: ^{13}C NMR spectrum of $BzSiCl_3$ post-sulfonation (400 MHz, $CDCl_3$, 23 °C)

Part 3: Crosslinking into the Solid Support Matrix

As previously discussed, the crosslinking process requires three components: (1) The solid support (in this case, the tin cube), (2) the linking agent, and (3) the linking reaction. The trimethyltin cube offers several advantages as a solid support: the silicon oxide framework makes for a robust support material resistant to both chemical influence from ligands attached to the dispersed silicon anchor points from the linking agents as well as the sometimes extreme thermal conditions associated with catalysis. Additionally, the metathesis linking reaction is simple and easily facilitated to maintain controlled formation of a single reaction product. This helps prevent the introduction of varying types of active sites both during synthesis and during catalysis that may lead to multiple reaction products, which would reduce product selectivity and introduce undesirable compounds in the reaction mixture.

Thus, the customization of this tailored catalyst will be controlled by variability in the linking agent used, and several variations will be tested to observe their effects on the products and their catalytic activity. Characterization of the reaction products at this point becomes more difficult, as we must rely on indirect methods to observe the changes in the solid heterogeneous catalyst. It is easiest to observe the primary degree of success of the cross-linking reactions by paying attention to gravimetric changes, analysis of volatile products released as a result of the cross-linking metathesis reaction, as well as a specific surface area (SSA) measurement of the solid products. These observations are presented in Table 1 below:

Table 1: Linking Reaction parameters and analysis of HSO_3-$BzSiCl_3$ with TMT Cube

Linker	Solvent	Temp	Ratio (Linker:Cube)	Grav (Max=3.0)	SSA (m^2/g)	Volatiles	Sample ID
HSO_3-$BzSiCl_3$	Toluene	RT	2:1	1.29	0.00	Me_3SnCl	**1A**
HSO_3-$BzSiCl_3$	Py	70 °C	2:1	1.12	5.32	Mixture	**1B**
HSO_3-$BzSiCl_3$	MeCN	RT	2:1	3.53	32.93	Me_3SnCl	**1C**
HSO_3-$BzSiCl_3$	MeCN	60 °C	2:1	1.33	58.16	Me_3SnCl	**1D**
HSO_3-$BzSiCl_3$	MeCN	60 °C	3:1	1.67	126.36	Me_3SnCl	**1E**
HSO_3-$BzSiCl_3$	MeCN	60 °C	4:1	1.71	7.91	Mixture	**1F**

The linking agent is created by reacting benzyltrichlorosilane, $BzSiCl_3$, with sulfonic acid, HSO_3, in order to sulfonate the para position of the benzyl ring, yielding HSO_3-$BzSiCl_3$. Since this compound is insoluble in methylene chloride, CH_2Cl_2; a few other solvents were investigated when reacting the linker with TMT cube until acetonitrile, MeCN, at 60 °C appeared to yield the most favorable results (samples **1D**, **1E;** Table 1).

A sample of the volatiles removed from the reaction product under vacuum can also be analyzed to determine what byproducts were produced. The most convenient method to do so is a simple ^1H NMR,

where the peak for trimethyltin chloride can be observed far upfield in the spectrum. If it is the only observable NMR signal, then Me_3SnCl is the only liberated volatile byproduct, which must be assumed for the gravimetric calculation. A mixture of products in the volatiles indicates that an undesirable reaction may have occurred and that the gravimetric calculation may not be accurate.

By keeping track of the weight changes between the reactants and formation of the products, an estimation of the trimethyltin chloride, Me_3SnCl, lost as a volatile can be calculated with respect to the number of moles of linker added. This will allow for determination of how many chlorides on the linker have reacted. Finally, since a high surface area (SSA) is correlated with catalytic activity, the stoichiometric ratio of linker:cube was adjusted between experiments to achieve a maximum SSAFollowing the previous rationale, several experiments were set up to test the linking of 1-dichloromethylsilylpropyl-3-benzylimidazolium chloride (1-DCMSP-3-Bz-Im Cl) with the TMT cube. The results of those reactions are presented in the Table 2 below:

Table 2: Linking Reaction parameters and analysis of 1-DCMSP-3-Bz-Im Cl with TMT Cube

Linker	Solvent	Temp	Ratio (Linker:Cube)	Grav (Max=2.0)	SSA (m^2/g)	Volatiles	Sample ID
1-DCMSP-3-Bz-Im Cl	CH_2Cl_2	RT	4:1	0.30	0.65	Mixture	**2A**
1-DCMSP-3-Bz-Im Cl	C_2HCl_3	60 °C	2:1	0.25	0.00	Me_3SnCl, H_2O	**2B**
1-DCMSP-3-Bz-Im Cl	C_2HCl_3	60 °C	3:1	0.33	0.00	Me_3SnCl, H_2O	**2C**
1-DCMSP-3-Bz-Im Cl	C_2HCl_3	60 °C	4:1	1.35	0.00	Me_3SnCl	**2D**
1-DCMSP-3-Bz-Im Cl with Py scavenger	C_2HCl_3	60 °C	4:1	1.38	0.00	Me_3SnCl	**2E**
1-DCMSP-3-Bz-Im Cl	MeCN	60 °C	2:1	0.41	0.00	Me_3SnCl	**2F**
1-DCMSP-3-Bz-Im Cl	MeCN	60 °C	3:1	0.28	0.00	Me_3SnCl	**2G**
1-DCMSP-3-Bz-Im Cl	MeCN	60 °C	4:1	0.00	1.05	Me_3SnCl	**2H**

These reactions proved to be more perplexing, as expected with increased complexity of the linking agent. While the volatiles often showed release of only Me_3SnCl, a significant surface area was never obtained with this linking agent. This suggests it is beneficial to crosslink with the HSO_3-$BzSiCl_3$ first to try and develop some surface area, followed by a second crosslinking with 1-DCMSP-3-Bz-Im Cl to add the ionic liquid functionality desired in the bifunctional catalyst (Table 3, below).

Table 3: Linking Reaction parameters and analysis of multiple functionalities with TMT Cube

Linker	Solvent	Temp	Ratio (Linker:Cube)	SSA (m^2/g)	Volatiles	Reference
1D + 2D	$MeCN/C_2HCl_3$	60 °C	3:1/4:1	0.46	Mixture	**3A**

Part 4: Catalysis Testing with Model Cellulosic Feedstock

In order to validate the use of the bifunctional heterogeneous catalyst, the performance of at least three linking agents must be tested: **(1)** HSO_3-R only **(2)** ionic liquid (IL) only **(3)** HSO_3- R and IL. However, it will also be ideal to compare this catalyst to the concentrated acid method that has commonly been employed in the conversion of biomass. Thus, the effect of a homogeneous concentrated acid, such as HCl or H_2SO_4 should be tested both with and without the presence of an ionic liquid affecting solubility of the reactants. This will add **(4)** concentrated acid only and **(5)** concentrated acid + free IL to the list of catalysis scenarios to be tested.

Catalysis testing utilized glucose (Glu) and cellobiose (CB), a dimer of glucose, as substrates. These compounds were chosen given that they are expected to be seen during the degradation of cellulosic biomass, yet have a less complex structure to help in the interpretation of reaction products.

Catalysis reactions were setup in a thick glass-walled pressure tube with a screw on O-ring cap in air, their contents detailed in Tables 3 and 4 further below. When the reactant, catalyst, and solvent had all been combined in the pressure tube, it was sealed and immersed in an oil bath at 80 °C overnight. Hot filtration through a frit was performed to separate solid and liquid reaction products, where the only expected solid would be the catalyst employed in the reaction. An aliquot of the liquid products were then analyzed on a Bruker 400 MHz solution state NMR in D_2O to see what changes had occurred between reactants and products. Of particular interest were hydroxymethylfurfural (HMF) from the degradation of glucose, as well as levulinic acid (LA) and formic acid (FA) from the hydrolysis of HMF. Characteristic ^1H signatures include: HMF δ [$CDCl_3$]: 9.53 (s), 7.23 (s), 6.52 (s), 4.69 (s), 3.73 (s). LA δ [$CDCl_3$]: 10.40 (b), 2.77 (d), 2.61 (d), 2.21 (s). FA δ [D_2O]: 8.26 (s)[40]. Several variations in the reaction mixture were chosen to elucidate the parameter responsible for the observed changes. Collected spectra for the observed products are displayed below, arranged by the catalyst applied to that particular set of reactions (see Tables 1 and 2 above).

i. Reference spectra of glucose and cellobiose

a. Glucose in D_2O

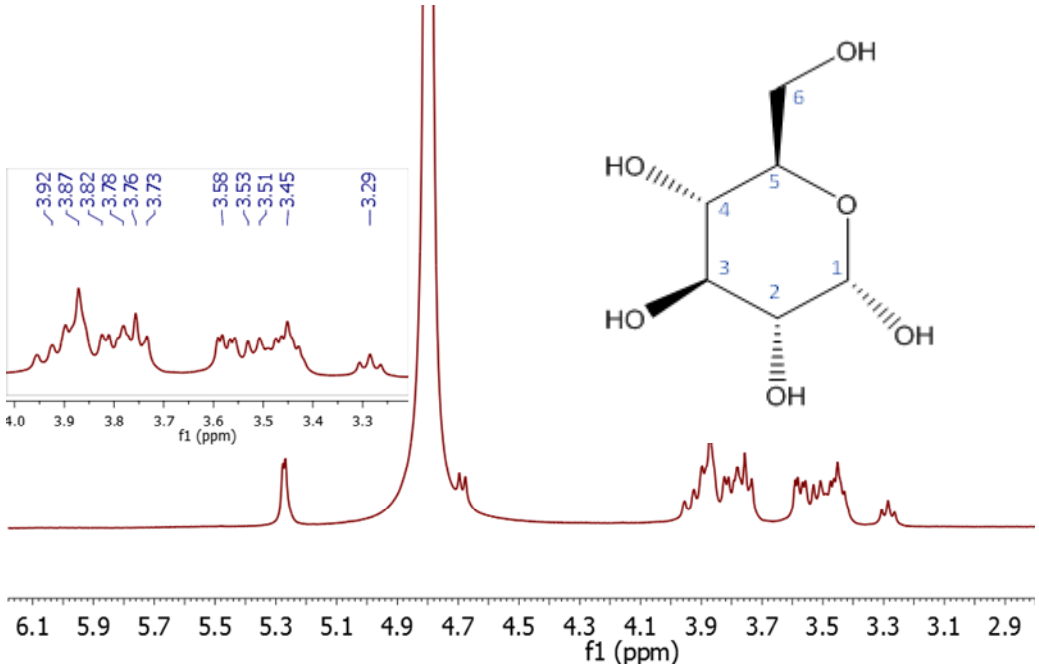

Figure 39: ^{1}H NMR spectrum of Glucose (400 MHz, D_2O, 23 °C)

The spectra of glucose shows a low chemical shift dispersion from the range δ = 3.3 - 4.0 due to the similarity of the shielding experienced by the protons in this structure, where those in the ring structure are closer to 3.3, and those on the alcohol functionalities are closer to 4.0. A large solvent water peak appears at δ = 4.8, with the unique peaks appearing around δ = 5.3 and δ = 4.7 attributed to the most deshielded proton in the anomeric C-1 position. The peaks at 4.7 ppm are contributed by the β-glucose anomer displayed in Figure 6, where the proton is more shielded in an axial position with respect to the ring and thus appears further upfield. Likewise, the signal at 5.3 ppm is assigned to the α-glucose anomer, where the proton is more deshielded in the equatorial position and is shifted further downfield.

Table 4: Assignment of fingerprint ^{1}H NMR chemical shifts for glucose[41]

α-D-Glu	β-D-Glu
α-H_1 ≈ 5.32 ppm	β-H_1 ≈ 4.74
	β-H_2 ≈ 3.37

b. Cellobiose in D_2O

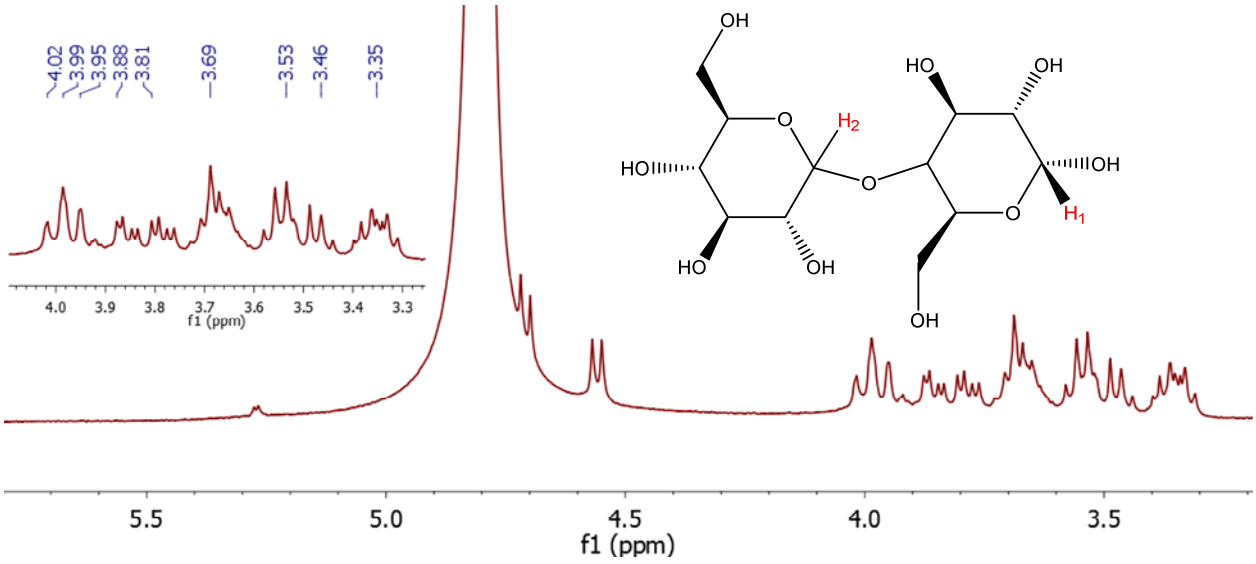

Figure 40: ^{1}H NMR spectrum of Cellobiose (400 MHz, D_2O, 23 °C)

Figure 41 shows a spectrum for cellobiose with many similarities to glucose. Noteworthy differences include a more complex series of peaks in the δ = 3.2 – 4.1 range and the absence of a resolved triplet at 3.3 ppm. Since the triplet is not seen for cellobiose, it may be used to detect formation of glucose from cellobiose. Additionally, the H_1 proton appears at δ = 5.3 and δ =4.7 resulting from either the α or β anomer, respectively. Finally, the H_2 proton contributes a unique doublet at 4.5 ppm.

Table 5: Assignment of fingerprint ^{1}H NMR chemical shifts for cellobiose[42]

α-D-Glu	β-D-Glu
α-H_1 ⍰ 5.24 ppm	β-H_1 ⍰ 4.67
α-H_2 ⍰ 4.52 ppm	β-H_2 ⍰ 4.52

ii. **Table 6:** Aqueous reactions of Glu and CB with **1E**

Feedstock	**Catalyst**	**Solvent**
97 mg Cellobiose	29 mg **1E**	5.290 g H_2O
200 mg Glucose	30 mg **1E**	5.132 g H_2O

a. Glu with **1E** in water, 80 °C, D_2O

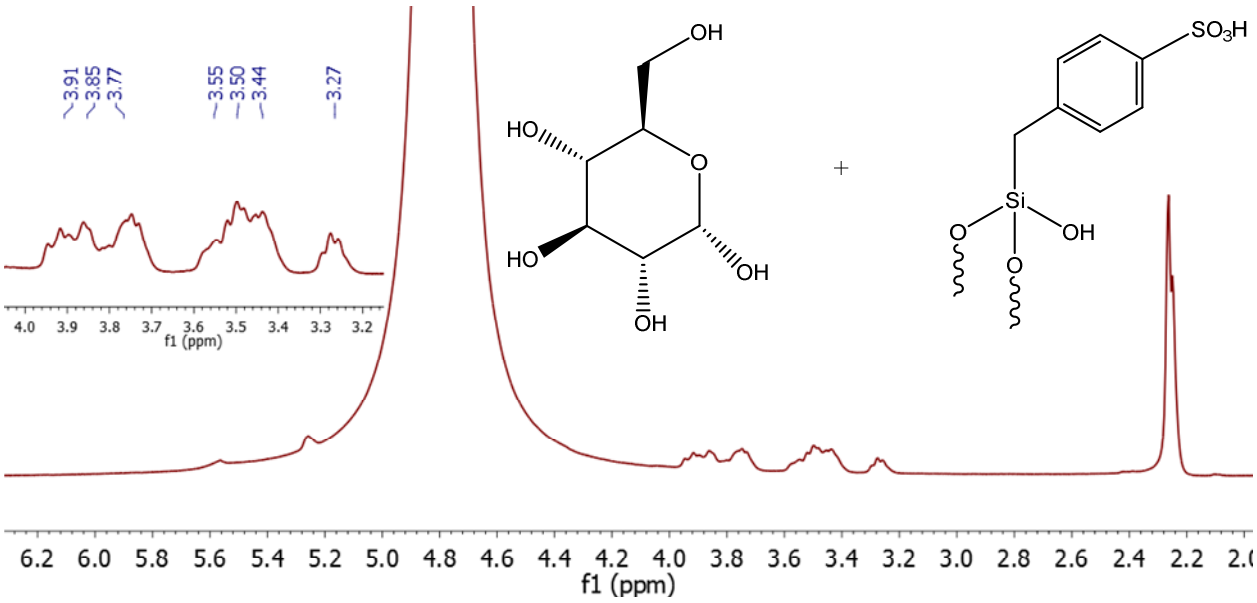

Figure 41: ^{1}H NMR spectrum of Glucose with 1E in water, 80 °C (400 MHz, D_2O, 23 °C)

When exposed to the sulfonic acid only catalyst, an aliquot from an aqueous suspension of glucose at 80 °C yields the spectrum shown in Figure 42 above. With exposure to the catalyst platform **1E**, it appears as though the doublet at δ = 4.7 corresponding to β-glucose has been replaced by a small peak at δ =

5.6. This may be a result of the β-glucose H_1 peak being masked by the large D_2O signal at δ = 4.8 (acetone also appears at δ = 2.3), or from equilibrium shifting unfavorably from β-glucose to α-glucose. Most importantly, the new peak appearing at δ = 5.6 does not correspond to any of the desired products, and no explicit downfield signals assignable to HMF, LA, or FA were observed.

b. CB with **1E** in water, 80 °C, D_2O

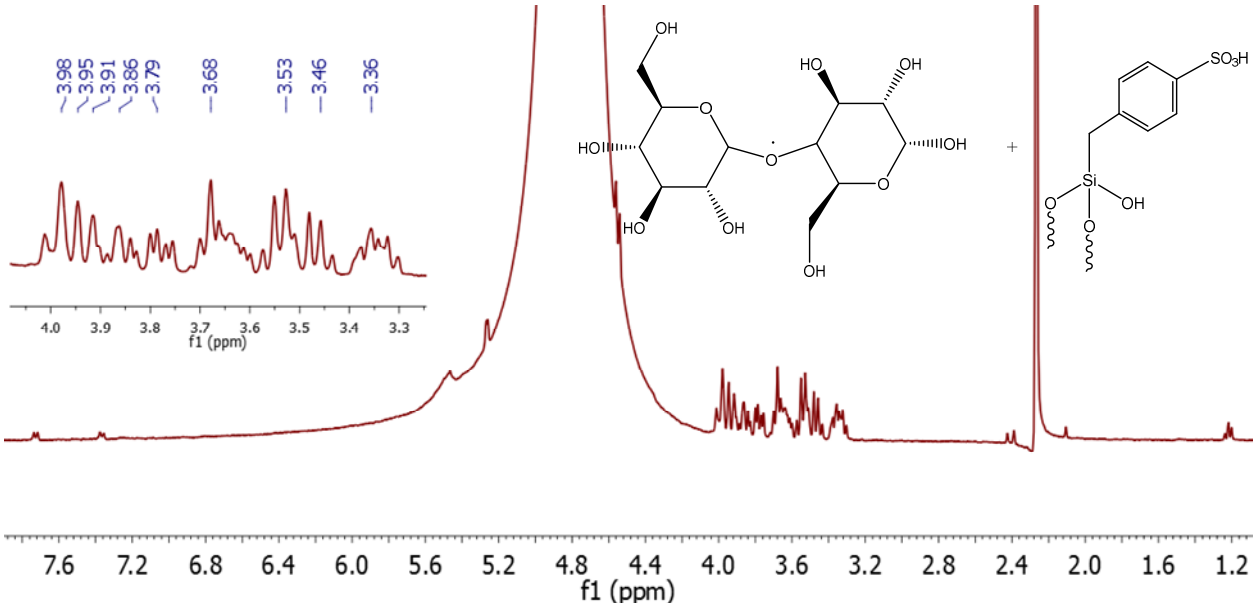

Figure 42: ^{1}H NMR spectrum of Cellobiose with 1E in water, 80 °C (400 MHz, D_2O, 23 °C)

These reaction parameters did not elicit any noticeable changes in the 3.2-4.1 region, however the rest of the spectrum shows differences similar to those observed when glucose was exposed to **1E**. This includes disappearance (or masking) of a δ = 4.7 peak corresponding to β-glucose, and the appearance of a new feature at δ = 5.5. Additionally, there is evidence of cleavage of an aromatic ring from the catalyst, indicated by two small doublets upfield of 7.0 that are characteristic of a para-substituted ring system, suggesting that the silane–acid functionality linkage has been severed.

iii. **Table 7:** Aqueous reactions of Glu and CB with **3A (1D + 2D)**

Feedstock	Catalyst	Solvent
109 mg Cellobiose	36 mg **3A**	5.102 g H_2O
202 mg Glucose	29 mg **3A**	5.315 g H_2O

a. Glu with **3A** in water, 80 °C, D_2O

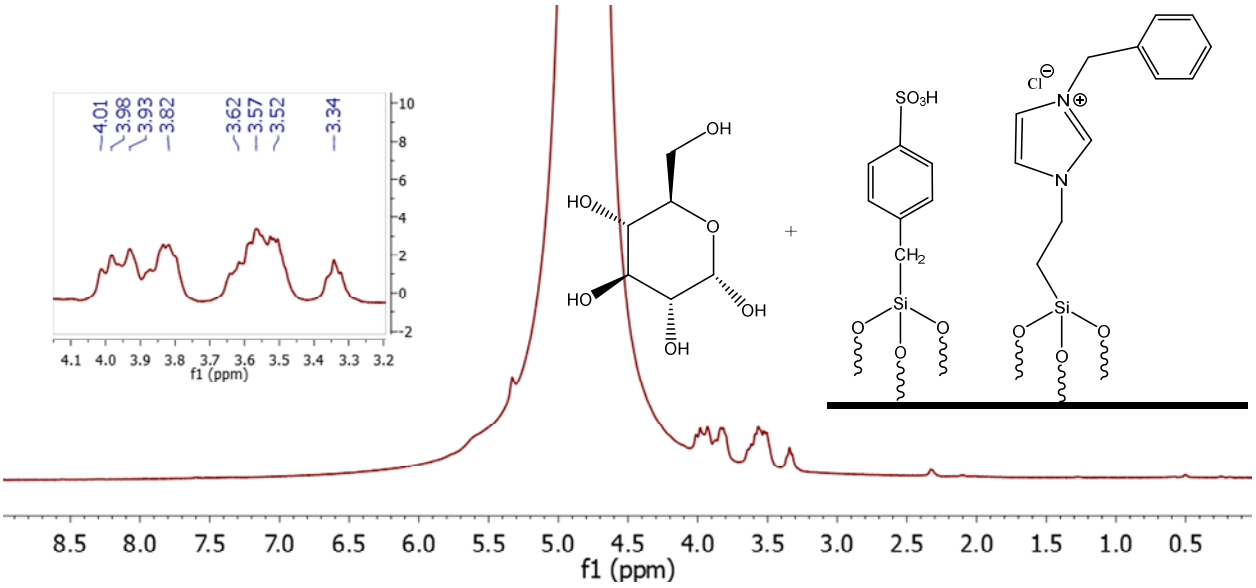

Figure 43: ^{1}H NMR spectrum of Glucose with 3A in water, 80 °C (400 MHz, D_2O, 23 °C)

The region of 3.3 – 4.0 ppm remains largely unchanged at this resolution, including the triplet appearing at δ = 3.3. Again, the β-glucose δ = 4.7 peak has disappeared and is accompanied by the appearance of a peak at δ = 5.6. A multitude of smaller peaks appear in the region of 0.0 – 2.2 ppm (Figure 44) that cannot confidently be assigned from these data. Again, no signals from HMF, LA, or FA were observed.

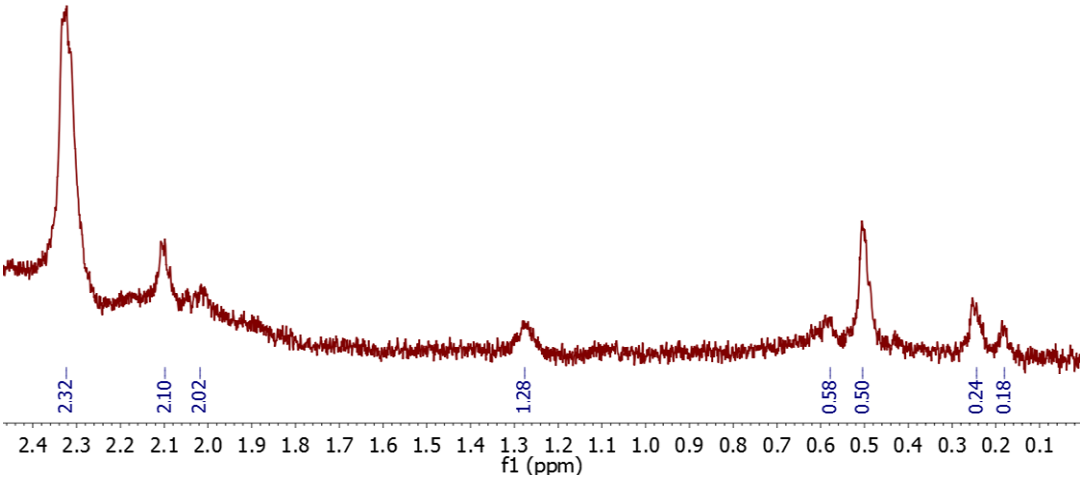

Figure 44: Expanded downfield region of ^{1}H NMR spectrum from Figure 44.

b. CB with **3A** in water, 80 °C, D_2O

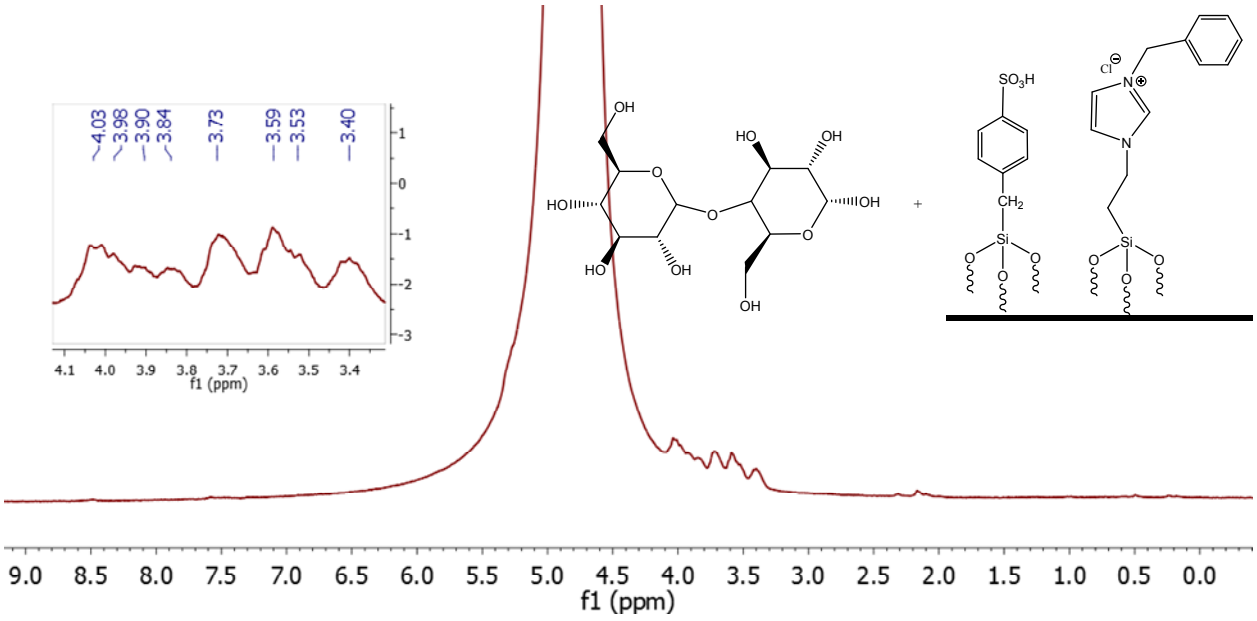

Figure 45: ^{1}H NMR spectrum of Cellobiose with 3A in water, 80 °C (400 MHz, D_2O, 23 °C)

The changes for cellobiose with the bifunctional catalyst again resemble those observed with sulfonic acid only (Figure 43). That is, the peaks from 3.3 – 4.0 ppm seem unchanged and several smaller peaks have formed in the 0 – 2.5 ppm region (Figure 46, below). The peak at δ = 3.4 may be a triplet corresponding to formation of glucose from cellobiose, but that conclusion is not certain at this resolution.

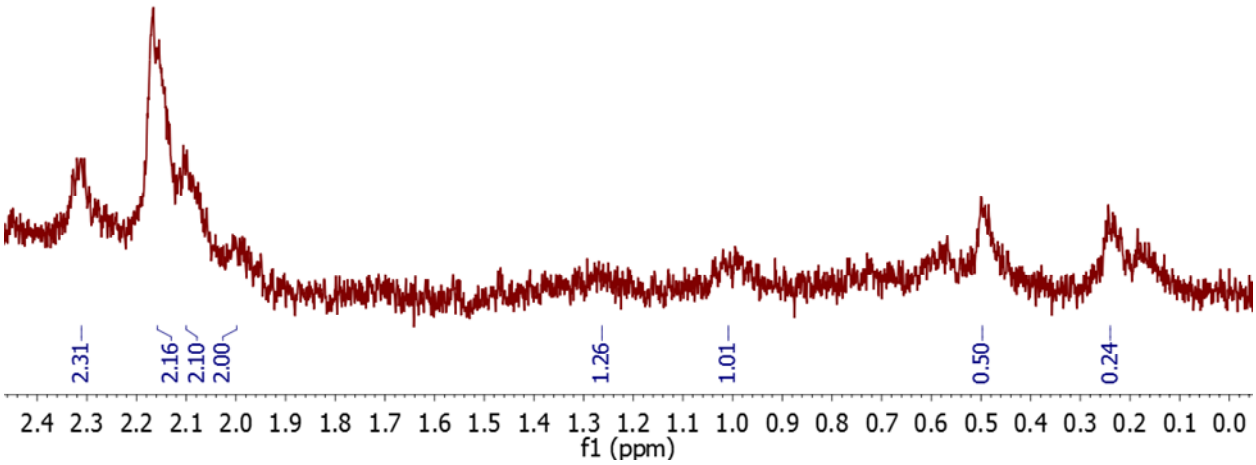

Figure 46: Expanded downfield region of ^{1}H NMR spectrum from Figure 46

Chapter 5: Conclusions

Through basic organo-metallic reactions, we have demonstrated the ability to synthesize a variety of chlorosilane linkers with either ionic liquid or sulfonic acid functionalities. However, the synthesis of a bifunctional linker utilizing imidazolium remains elusive. Additionally, while there is indirect evidence for the incorporation of these silanes into the porous matrices derived from the trimethyltin cube. Characterization of the resulting solid is not complete.

Catalysis testing of the model lignocellulosic compounds cellobiose and glucose showed varied results. Exposure of these substrates to a heterogeneous catalyst containing only acid showed no change to the alcohol functionalities of the cyclic carbohydrates and failed to indicate the formation of hydroxymethylfurfural, levulinic acid, or formic acid as products of hydrolysis.

Furthermore, catalysis testing of a platform containing both ionic liquid and acidic functionalities under identical conditions did show evidence for some product formation, however the compounds formed could not be identified by ^{1}H NMR on a 400 MHz alone.

Future work includes a more in depth characterization of the resulting heterogeneous catalyst including IR spectroscopy and solid state NMR (SSNMR). Additionally, GC-MS would be a valuable tool to try and resolve what products were formed in the reaction mixture. Finally, assuming an ideal catalyst containing both acidic and ionic liquid functionalities could be created and proved effective at the conversion of lignocellulosic biomass, it would be beneficial to study to reuse of the catalyst for multiple reaction cycles.

List of References

1. Micromeritics, Characterization of acid sites using temperature-programmed desorption. Application Note 2003; Vol. 134, pp 1-5.
2. EIA. Annual Energy Outlook 2012 with Projections to 2035 2012. www.eia.gov/forecasts/aeo.
3. Bryan, P. The How's and Why's of Replacing the Whole Barrel 2011. http://energy/gov/articles/hows-and-whys-replacing-whole-barrel (accessed 07/30/12).
4. EIA Top World Oil Producers, Consumers, Imports, and Exports, 2011. www.eia.gov/countries/ (accessed 07/30/12).
5. DOE Strategic Petroleum Reserve - Profile. www.fossil.energy.gov/programs/reserves/spr/index.html (accessed 07/30/12).
6. IEA. From 1st- to 2nd-Generation Biofuel Technologies 2008. http://www.iea.org/papers/2008/2nd_Biofuel_Gen.pdf (accessed 08/10/2012).
7. Li, H.; Foston, M. B.; Kumar, R.; Samuel, R.; Gao, X.; Hu, F.; Ragauskas, A. J.; Wyman, C. E., Chemical composition and characterization of cellulose for Agave as a fast-growing, drought-tolerant biofuels feedstock. *RSC Advances* **2012,** *2* (11), 4951.
8. Ogaki, Y.; Shinozuka, Y.; Hatakeyama, M.; Hara, T.; Ichikuni, N.; Shimazu, S., Selective Production of Xylose and Xylo-oligosaccharides from Bamboo Biomass by Sulfonated Allophane Solid Acid Catalyst. *Chemistry Letters* **2009,** *38* (12), 1176-1177.
9. IEA. Sustainable Production of Second-Generation Biofuels 2010. http://www.iea.org/papers/2010/second_generation_biofuels.pdf (accessed 08/10/2012).
10. Yarris, L. The Evolutionary Road to Biofuels 2010. http://www.lbl.gov/Publications/YOS/Feb/index.html (accessed 08/10/2012).
11. Binder, J. B. R., Ronald T., Simple Chemical Transformation of Lignocellulosic Biomass into Furans for Fuels and Chemicals. *JACS* **2009,** *131*, 1979-1985.
12. Himmel, M. V., T.; Bower, S.; Jechura, J., BSCL Use Plan: Solving Biomass Recalcitrance. *Technical Report* **2005,** *NREL/TP-510-37902*.
13. Mosier, N.; Wyman, C.; Dale, B.; Elander, R.; Lee, Y. Y.; Holtzapple, M.; Ladisch, M., Features of promising technologies for pretreatment of lignocellulosic biomass. *Bioresource technology* **2005,** *96* (6), 673-86.
14. Domańska, U., Solubilities and thermophysical properties of ionic liquids. *Pure and Applied Chemistry* **2005,** *77* (3), 543-557.
15. Rinaldi, R.; Palkovits, R.; Schuth, F., Depolymerization of cellulose using solid catalysts in ionic liquids. *Angew Chem Int Ed Engl* **2008,** *47* (42), 8047-50.
16. Ertl, G. K., H.; Schüth, F.; Weitkamp, J., *Handbook of Heterogeneous Catalysis*. Wiley-VCH: Weinheim, 2008; Vol. 1.
17. Rinaldi, R.; Schüth, F., Design of solid catalysts for the conversion of biomass. *Energy & Environmental Science* **2009,** *2* (6), 610.
18. King, G. J., Ullmann's Encyclopedia of Industrial Chemistry. Weinheim, 2007.
19. Bobleter, O. Hydrothermal Degradation and Fractionation of Saccharides and Polysaccharides *Polysaccharides* [Online], 2004.
20. Onda, A.; Ochi, T.; Yanagisawa, K., Selective hydrolysis of cellulose into glucose over solid acid catalysts. *Green Chemistry* **2008,** *10* (10), 1033.
21. Dutta, A.; Patra, A. K.; Dutta, S.; Saha, B.; Bhaumik, A., Hierarchically porous titanium phosphate nanoparticles: an efficient solid acid catalyst for microwave assisted conversion of biomass and carbohydrates into 5-hydroxymethylfurfural. *Journal of Materials Chemistry* **2012,** *22* (28), 14094.
22. Peng, L.; Lin, L.; Li, H.; Yang, Q., Conversion of carbohydrates biomass into levulinate esters using heterogeneous catalysts. *Applied Energy* **2011,** *88* (12), 4590-4596.

23. Amarasekara, A. S.; Owereh, O. S., Synthesis of a sulfonic acid functionalized acidic ionic liquid modified silica catalyst and applications in the hydrolysis of cellulose. *Catalysis Communications* **2010,** *11* (13), 1072-1075.
24. Illanes, A. Z., M. E.; Contreras, S.; Guerrero, A., Reactor Design for the Enzymatic Isomerization of Glucose to Fructose. *Bioprocess Engineering* **1992,** *7* (5), 199-204.
25. Watanabe, M.; Aizawa, Y.; Iida, T.; Nishimura, R.; Inomata, H., Catalytic glucose and fructose conversions with TiO2 and ZrO2 in water at 473K: Relationship between reactivity and acid–base property determined by TPD measurement. *Applied Catalysis A: General* **2005,** *295* (2), 150-156.
26. Qi, X.; Watanabe, M.; Aida, T. M.; Smith Jr, R. L., Catalytical conversion of fructose and glucose into 5-hydroxymethylfurfural in hot compressed water by microwave heating. *Catalysis Communications* **2008,** *9* (13), 2244-2249.
27. Zhao, H.; Holladay, J. E.; Brown, H.; Zhang, Z. C., Metal chlorides in ionic liquid solvents convert sugars to 5-hydroxymethylfurfural. *Science* **2007,** *316* (5831), 1597-600.
28. Franks, F., Physical chemistry of small carbohydrates - equilibrium solution properties. *Pure and Applied Chemistry* **1987,** *59* (9), 1189-1202.
29. Moliner, M.; Roman-Leshkov, Y.; Davis, M. E., Tin-containing zeolites are highly active catalysts for the isomerization of glucose in water. *Proceedings of the National Academy of Sciences of the United States of America* **2010,** *107* (14), 6164-8.
30. Chheda, J. N.; Huber, G. W.; Dumesic, J. A., Liquid-phase catalytic processing of biomass-derived oxygenated hydrocarbons to fuels and chemicals. *Angew Chem Int Ed Engl* **2007,** *46* (38), 7164-83.
31. Moreau, C. D., R.; Razigade, S.; Duhamet, J.; Faugeras, P.; Rivalier, P.; Ros, P.; Avignon, G., Dehydration of fructose to 5-hydroxymethylfurfural over H-mordenites. *Applied Catalysis A: General* **1996,** *145*, 211-224.
32. Kim, E. S.; Liu, S.; Abu-Omar, M. M.; Mosier, N. S., Selective Conversion of Biomass Hemicellulose to Furfural Using Maleic Acid with Microwave Heating. *Energy & Fuels* **2012,** *26* (2), 1298-1304.
33. Tanabe, K. H., W., Industrial application of solid acid-base catalysts. *Applied Catalysis A: General* **1999,** (181), 399-434.
34. Ramos, L. P., The chemistry involved in the steam treatment of lignocellulosic materials. *Quim. Nova* **2003,** *26* (6), 863-871.
35. Fukuoka, A.; Dhepe, P. L., Catalytic conversion of cellulose into sugar alcohols. *Angew Chem Int Ed Engl* **2006,** *45* (31), 5161-3.
36. Luo, C.; Wang, S.; Liu, H., Cellulose conversion into polyols catalyzed by reversibly formed acids and supported ruthenium clusters in hot water. *Angew Chem Int Ed Engl* **2007,** *46* (40), 7636-9.
37. Badley, R. D. F., W. T., Silica-Bound Sulfonic Acid Catalysts. *J. Org. Chem.* **1989,** (54), 5437-5443.
38. Tao, F.; Song, H.; Chou, L., Hydrolysis of cellulose in SO3H-functionalized ionic liquids. *Bioresource technology* **2011,** *102* (19), 9000-6.
39. Parambadath, S.; Chidambaram, M.; Singh, A. P., Synthesis, characterization and catalytic properties of benzyl sulphonic acid functionalized Zr-TMS catalysts. *Catalysis Today* **2004,** *97* (4), 233-240.
40. AIST Spectral Database for Organic Compounds SDBS. http://sdbs.riodb.aist.go.jp (accessed 10/19).
41. Pomin, V. H., Glycosylation. In *Unraveling Glycobiology by NMR Spectroscopy* [Online] Petrescu, S., Ed. Creative Commons, 2012. (accessed 10/29/2013).
42. Guo AC, J. T., Wilson M, Liu Y, Knox C, Djoumbou Y, Lo P, Mandal R, Krishnamurthy R, Wishart DS. ECMDB: The E. coli Metabolome Database. http://www.ecmdb.ca (accessed 10/31).

Vita

Matthew Dembo was born in Middleton, NY to the parents of Barry and Nancy Dembo. Shortly thereafter he moved to Virginia where he attended Riverbend High School in Spotsylvania, Virginia. After graduation in 2007, he continued his education nearby at The College of William and Mary in Williamsburg, Virginia. While there he developed an interest in neuroscience but continued with his participation in undergraduate research in chemistry by characterizing the luminescent properties of copper-amine coordination compounds. He obtained a Bachelors of Science for both his chemistry and neuroscience majors in May 2011 from William and Mary and started with a research opportunity for graduate students in June at the University of Tennessee, Knoxville. There he developed a specialization in inorganic chemistry while working on an alternative fuels project in biomass catalysis, and graduated with a Masters in chemistry in December 2013.